

UNIVERSITY OF CAPE COAST

THE EFFECTS OF TIME DELAY ON STAGE STRUCTURED MODEL WITH
MICHAELIS-MENTENS-TYPE HARVESTING



PRINCE BASIL AKPO

2023



© Prince Basil Akpo
University of Cape Coast

UNIVERSITY OF CAPE COAST

THE EFFECTS OF TIME DELAY ON STAGE STRUCTURED MODEL WITH
MICHAELIS-MENTENS-TYPE HARVESTING

BY

PRINCE BASIL AKPO

Thesis Submitted to the Department of Mathematics of the School of Physical
Sciences, College of Agriculture and Natural Sciences, University of Cape
Coast in partial fulfillment of the requirement for award of Master of
Philosophy degree in Mathematics

DECEMBER, 2023

DECLARATION

Candidate's Declaration

I hereby declare that this thesis is the result of my own original research and no part of it has been presented for another degree in this University or elsewhere.


Candidate's Signature 

Date 04-08-2025

Name: PRINCE BASIL AKPO

Supervisor's Declaration

I hereby declare that the preparation and presentation of the thesis were supervised in accordance with the guidelines on supervision of thesis laid down by the University of Cape Coast .

Supervisor's Signature 

Date 04-08-2025

Name: PROF. MARTIN ANOKYE

ABSTRACT

This research work investigate the effect of time delay on the stage structured model with Michaelis-Mentens-type harvesting. The study proved the existence of all potential equilibria of the system. However, the analysis was concentrated on coexistence equilibrium E_* to establish its stability at $\tau = 0$. For $\tau > 0$, the stability switch and associated Hopf bifurcation were proved. This characteristics were not found in the previous work. Numerical simulations were done using Matlab to confirm the dynamics of the analytic solution.

KEY WORDS

Asymptotic Stability

Hopf Bifurcation

Positive Steady State

Saddle Node Bifurcation

Stability Switch

Transversal Condition

ACKNOWLEDGEMENTS

I wish to express my profound gratitude to Almighty God for his direction, favour and blessings upon my life.

I am really grateful to my supervisor, Prof. Martin Anokye, for his help, advice and insightful comments during the writing process. His knowledge and support have been invaluable in helping me shape this thesis.

To my family and friends, who have helped me through all of the highs and lows of this academic journey with their unfailing support and encouragement. Your confidence in me has kept me going and I sincerely appreciate your love and support.

DEDICATION

To my wife, Mrs. Joy Schlliegel-Akpo.

My Children Mawulorm, Edudzi and Mawuenam

TABLE OF CONTENTS

	Page
DECLARATION	ii
ABSTRACT	iii
KEY WORDS	iv
ACKNOWLEDGEMENTS	v
DEDICATION	vi
LIST OF TABLES	ix
LIST OF FIGURES	x
CHAPTER ONE: INTRODUCTION	
Background to the Study	1
Statement of Problem	9
General Objectives	9
Specific Objectives	10
Assumption of the Model	10
Significant of the study	10
Delimitations	11
Limitations	11
Definition of Terms	11
Organization of the Study	14
CHAPTER TWO: LITERATURE REVIEW	
Introduction	15
Brief History on Model	15
Chapter Summary	21

CHAPTER THREE: RESEARCH METHODS	
Introduction	23
Stability Analysis	24
Non-Delay structure Model Without Harvesting	25
Delay structure Model Without Harvesting	27
Delay Functional Response Model	31
Stability Analysis when $\tau = 0$	33
Stability Analysis when $\tau \neq 0$	34
Chapter Summary	44
CHAPTER FOUR: RESULTS AND DISCUSSIONS	
Introduction	45
Numerical and Hopf-Bifurcation Analysis	45
Chapter Summary	61
CHAPTER FIVE: SUMMARY, CONCLUSIONS AND RECOMMENDATIONS	
Overview	62
Summary	62
Conclusions	64
Recommendations	65
REFERENCE	65
APPENDIX: MATLAB CODES FOR THE PROJECT	68

LIST OF TABLES

	Page
1 Existing Parameters	23
2 Existing Parameters and Value	46
3 New Parameters and Value	50

LIST OF FIGURES

	Page
1 Phase portrait of model (21), $\alpha=1, \beta=0.75, \gamma=4, \delta_1=0.26, \delta_2=0.25$	47
2 Simulation of model (21), $\alpha=1, \beta=0.75, \gamma=4, \delta_1=0.26, \delta_2=0.25$	47
3 Phase portrait of model (22), $\alpha=1, \beta=0.75, \gamma=4, \delta_1=0.26, \delta_2=0.25, \tau=0.2$	48
4 Phase portrait of model (22), $\alpha=1, \beta=0.75, \gamma=4, \delta_1=0.26, \delta_2=0.25, \tau=0.5$	49
5 Phase portrait of model (22), $\alpha=1, \beta=0.75, \gamma=4, \delta_1=0.26, \delta_2=0.25, \tau=0.8$	49
6 Simulation of model (22), $\alpha=1, \beta=0.75, \gamma=4, \delta_1=0.26, \delta_2=0.25, \tau=0.8$	50
7 Phase portrait of model (23), $a=1, b=0.75, c=0.26, e=4$	51
8 Phase portrait of model (24), $a=1, b=0.75, c=0.26, e=4, \tau=0.2$	52
9 Phase portrait of model (24), $a=1, b=0.75, c=0.26, e=4, \tau=0.8$	52
10 Phase portrait of model (23), $a=1, b=20/27, c=7/27, e=4$	53
11 Phase portrait of model (24), $a=1, b=20/27, c=7/27, e=4, \tau=0.2$	54
12 Phase portrait of model (24), $a=1, b=20/27, c=7/27, e=4, \tau=0.8$	54
13 Simulation of model (23) $a=1, b=0.25, c=0.125, e=0.5$	55
14 Simulation of model (24) $a=1, b=0.25, c=0.125, e=0.5, \tau=0.2$	56
15 Simulation of model (24) $a=1, b=0.25, c=0.125, e=0.5, \tau=0.8$	56
16. Simulation of model (23) $a=1, b=1, c=12, e=2$	57

17 Simulation of model (24) $a=1, b=1, c=12, e=2, \tau=0.2$	57
18 Simulation of model (24) $a=1, b=1, c=12, e=2, \tau=0.8$	58
19 Phase portrait of model (24), $a=1, b=0.25, c=0.125, e=0.5, \tau=4.71$	58
20 Simulation of model (24), $a=1, b=0.25, c=0.125, e=0.5, \tau=4.71$	59

CHAPTER ONE

INTRODUCTION

Harvesting is the process of gathering plants and animals for sustenance. In the framework of the predator-prey paradigm, harvesting refers to the interdependence of many organisms within an ecosystem. This dependency is followed by the interactions between the various animals with respect to food and survival for life (Yu *et al.*,2020).

Harvesting activities include fishing, hunting, or trapping certain prey species, in addition to managing or eliminating predator populations (Lennox *et al.*, 2022).

The stability of ecosystems and the dynamics of predator-prey relationships can be significantly impacted by harvest. It can change predator-prey populations' distribution and abundance, as well as their behaviors and ecological functions within the ecosystem. Sustainable harvesting methods seek to satisfy human needs and preserve biodiversity while preserving the equilibrium between predator-prey populations.

In the predator-prey model system, certain species are considered food, referred to as prey, and those who take advantage of the weaker or more susceptible animals for sustenance are referred to as predators.

Background to the Study

The terms "constant yield harvesting" and "constant effort harvesting" refer to the two different methods of harvesting, according to (May *et al.*, 1979). The former is characterized by a continuous harvest, independent of population growth. The prey population is therefore collected at a constant rate h , regardless of population size x , as indicated by:

$$H(x,t) = h. \tag{1}$$

Although it makes sense when x is high, the assumption of a constant harvesting rate h becomes less when x is small.

In contrast, the latter is referred to as proportionate harvesting and is characterized by a continuous multiplication of the population that is being harvested. In this case, the availability of prey within the ecosystem determines how it is harvested. That is, it makes sense to assume that for a given level of effort, the population x determines how quickly the prey are harvested. Therefore, it is easier to harvest more prey when there is more of it. Another way to represent the harvest rate is as follows:

$$H(x,t) = Ex, \quad (2)$$

where E , a positive constant expressed in units $1/time$, represents the total effort required to collect the specified prey.

Linear harvesting includes constant yield harvesting. In this case, its expression has the form $H = qEx$, (May *et al.*, 1979). Here q is the catchability coefficient.

Clark and Mangel (1979), also proposed nonlinear harvesting, which refers to harvesting strategies, where the rate or intensity of harvesting is not constant but varies with changes in the population size. This also includes constant effort harvesting.

Since harvesting is not constant, it can lead to threshold effects. That is, the structure and function of ecosystems can be disproportionately affected by slight changes in harvesting intensity if specific thresholds are crossed.

The Michaelis-Menten-type harvesting model is an example of non-linear harvesting, which is in the form:

$$H = \frac{qEx}{mE + nx}, \quad (3)$$

where the parameter h is harvesting rate (the rate at which resources are har-

vested), q is catchability coefficient (a measure of how easily the resource can be harvested), E is effort (the amount of resources used for harvesting, such as the number of fishing vessels), x is stock density (population size), m is maximum harvesting rate (the maximum rate at which resources can be harvested), n is half-saturation constant (the stock density at which the harvesting rate is half of the maximum harvesting rate).

In this context, the equation describes how the harvesting rate h changes in response to changes in effort E and stock density x . The equation represents a non-linear relationship between harvesting rate and effort, with the harvesting rate saturating at high effort levels. The model is used to manage resources sustainably, understanding the impact of harvesting on population dynamics, and setting optimal harvesting levels.

Many academics have used the two harvesting models that have been suggested to determine the interactions that exist between the species in their ecosystem. Using the linear harvesting system, (Xiao & Lei, 2018) examined how harvesting affected the dynamics of a stage structure model for a single species. The model's shape is:

$$\begin{aligned}\frac{dx_1}{dt} &= \alpha x_2 - \beta x_1 - \delta_1 x_1 - q_1 E m x_1, \\ \frac{dx_2}{dt} &= \beta x_1 - \delta_2 x_2 - \gamma x_2^2 - q_1 E m x_2,\end{aligned}\tag{4}$$

where x_1 is the juvenile species density (the number of individuals per unit area/volume), x_2 is the adult species density (the number of individuals per unit area/volume), α is the growth coefficient (the rate at which juveniles grow into adults), β is the maturation rate (the rate at which juveniles mature into adults), δ_1 is the juvenile mortality rate (the rate at which juveniles die), δ_2 is the adult mortality rate (the rate at which adults die), γ is the competition coefficient (the rate at which adults compete for resources), q_1 is the harvesting

coefficient (the rate at which species is harvested), E is the harvesting effort (amount of resources used for harvesting), m is the maximum harvesting rate (the maximum rate at which species can be harvested).

The model describes the dynamics of a single species with two stages (juveniles and adults) and the impact of harvesting on the population. The equations represent changes in juvenile and adult densities over time, influenced by growth, maturation, mortality, competition, and harvesting.

The model is used to calculate sustainable harvesting strategies, such as resource availability, and to comprehend how harvesting affects population dynamics. Thus, if the rate of harvesting is lower than the resource's natural growth rate, it can be sustained over the long term. Means the resource population can replenish and remain available for future use.

If the harvesting exceeds the resource's natural growth rate, it can lead to over-harvesting. Then over time, this can deplete the resource availability, leading to resource collapse. Again, Economic factors, such as the demand for the resource and the cost of harvesting. Thus if the demand for the prey population is high, and the cost of harvesting is low, there may be the incentives for higher harvesting which can impact the resource.

The impact of Michael-Mentens-type harvesting regarding the amensalism model's dynamics with Cover was examined in Liu *et al.*(2018). The updated model has the following form:

$$\begin{aligned}\frac{dx}{dt} &= a_1x - b_1x^2 - c_1(1-k)xy - \frac{qE(1-k)x}{m_1E + m_2(1-k)x}, \\ \frac{dy}{dt} &= a_2y - b_2y^2,\end{aligned}\tag{5}$$

where, x is the prey species' (or harvested species') density. t represents time, y represents the density of the other species (non-harvested species), c_1 is the interaction coefficient between the two species (representing amensalism), a_1 is

the prey species' growth rate, b_1 is its intraspecific competition coefficient, k is the cover proportion (the percentage of habitat covered by the non-harvested species), and q is the harvesting coefficient (the rate at which the prey species is harvested), m_1 is the harvesting half-saturation constant (density at which the harvesting rate is half of the maximum), m_2 is the conversion factor (relates the harvesting rate to prey density), a_2 is the growth rate of the non-harvested species, and b_2 is the intraspecific competition coefficient of the non-harvested species. E is the harvest effort (or amount of resources used for harvesting).

The model depicts two species: those that are taken for food and those that provide cover, or a safe haven or shelter, to the prey species. The Michaelis-Menten-type harvesting model represents a nonlinear relationship between the rate of harvesting and the density of prey, from which the name "harvesting" is derived. The purpose of the model is to study the dynamics and stability of the two species during harvesting, as well as the resulting effects.

The harvesting process affects the ecosystem in the following ways since it is nonlinear: *population fluctuation*, thus, little is harvested while the prey population is low, allowing it to rebuild. However, higher harvesting rates have the potential to reduce the prey population once it passes a certain threshold, which would then have an impact on the predator population as well. As a result, it can result in oscillations or erratic dynamics in the population.

In addition, the population can show different degrees of resilience to outside shocks or environmental changes depending on the specifics of the harvesting role. In other words, it might increase or decrease population resilience.

Yu *et al.*(2020), also proposed the dynamic behavior of a single species stage structure model with juvenile population harvesting similar to Michaelis-Mentens. The form of the model is:

$$\begin{aligned}\frac{dx}{dt} &= \alpha y - \beta x - \delta_1 x - \frac{hEx}{mE + nx}, \\ \frac{dy}{dt} &= \beta x - \delta_2 y - \gamma y^2.\end{aligned}\tag{6}$$

where, α denotes the growth coefficient (the rate at which juveniles mature into adults), x represents the juvenile population density, y represents the adult population density, and t represents time. β is the maturation rate (the rate at which juveniles mature into adults), δ_1 is the juvenile mortality rate (the rate at which juveniles die), δ_2 is the adult mortality rate (the rate at which adults die), γ is the competition coefficient (the rate at which adults compete for resources), h is the harvesting coefficient (the rate at which juveniles are harvested), E is the harvesting effort (amount of resources used for harvesting), The conversion factor, n , links harvesting rate to the juvenile density, and m is the half-saturation constant for harvesting (the density at which the harvesting rate is half of the maximum).

The model illustrates the two-stage dynamics of a single species: juveniles and adults, as well as the effects of harvesting on the juvenile population. The Michaelis-Menten-type harvesting model serves as the foundation for the harvesting term, which represents a non-linear relationship between harvesting rate and juvenile density. This model is used to study the dynamic behaviour of the population and the effects of harvesting on the juvenile population.

The following is a summary of how Michaelis-Mentens-type harvesting affects the prey population: *threshold effect*, meaning that the harvest rate is comparatively low if the prey population x is smaller than m . But the harvest rate rises with the number of prey. In other words, when the population approaches the threshold m , the pressure to harvest the prey grows.

Additionally, *Ecosystem impact*, a shift in the prey population caused by this harvest function, may have repercussions that ripple through the ecosystem.

That is, since every organism depends on every other organism for life, a decline in the prey population may have an impact on predator numbers and other ecological relationships. Of the three suggested harvesting models, non-linear harvesting is usually more ecologically beneficial since it prioritizes preserving a sustainable population.

For example, fear effect is incorporated into the impact of Michaelis-Menten-type harvesting in a Lotka-Volterra predator-prey system, (Lai *et al.*, 2020). This has the following form:

$$\begin{aligned}\frac{dx}{dt} &= x\left(a - bx - \frac{fy}{x+k}\right) - \frac{hx}{mE + nx}, \\ \frac{dy}{dt} &= y(e - gy + sx),\end{aligned}\tag{7}$$

where prey population density is represented by x , predator population density by y , prey growth rate by a , and prey self-limitation coefficient by b . Predation rate f , half-saturation constant k , harvesting coefficient h , harvesting effort E , harvesting half-saturation constant m , conversion factor n , predator growth rate e , predator self-limitation coefficient g , and fear effect coefficient s are all represented.

The model showing the predator-prey system with Michaelis-Menten-type harvesting incorporates the fear effect, which postulates that the presence of predators has an influence on the prey population.

Furthermore, for all allowable initial densities of both species, there are critical harvesting values that, when exceeded by the harvest rate, result in the extinction of the predator species. By incorporating Michaelis-Menten type harvesting and a fear effect, the model becomes more biologically realistic, as it captures additional factors that influence predator-prey dynamics in natural ecosystems.

The model allows researchers to explore how these factors interact with each other and with the intrinsic dynamics of the system, leading to a deeper under-

standing of population dynamics and ecosystem stability. Their findings have implications for both theoretical ecology and real-world resource management, as they offer a useful framework for researching how predators and prey interact when harvesting and fear effects are present. Furthermore, the model's dynamical behavior is highly sensitive to non-linear harvesting, necessitating careful application of conservation, preservation, and management of renewable resources.

Lv *et al.* (2019), two predator-prey models with nonlinear harvesting, bifurcations, and simulations,

$$\begin{aligned}\frac{dx}{dt} &= x(1-x) - \frac{xy}{x+k} - \frac{hx^2}{mE + nx^2}, \\ \frac{dy}{dt} &= y(-a + bx),\end{aligned}\tag{8}$$

where, predator population density is y , and the prey population density is x . Predation rate is b , while the predator growth rate is a . Half-saturation constant for harvesting is m , the conversion factor is n , the harvesting coefficient is h , the harvesting effort is E , and the half-saturation constant for harvesting is k .

Model provides insights into how changes in system parameters (such as harvesting rates or prey fear responses) can lead to different types of behaviour, including stable equilibria, limit cycles, or chaotic dynamics. Their work allow for the investigation of how harvesting intensity and functional forms of harvesting rates influence the stability and behavior of predator-prey populations over time. It also offers a computational exploration of the dynamics predicted by their models. Through simulations, they observe how the system evolves over time under different conditions and parameter settings. This makes it possible to comprehend the long-term effects of nonlinear harvesting on predator-prey dynamics in greater detail. Last but not least, their research advances the knowledge of the intricate dynamics of predator-prey systems under the impact of

nonlinear harvesting, providing important new perspectives for both theoretical ecology and real-world conservation initiatives.

Statement of Problem

The study utilized model (6) and added a time delay parameter τ to the juvenile term to account for developmental time until they are ready for harvesting and to assess how the model's dynamics are impacted by the time delay. This is due to the fact that the body of current literature demonstrates that no research has been conducted using the form of model provided below:

$$\begin{aligned}\frac{dx}{dt} &= \alpha y - (\beta + \delta_1)x(t - \tau) - \frac{hEx}{mE + nx}, \\ \frac{dy}{dt} &= \beta x - \delta_2 y - \gamma y^2.\end{aligned}\tag{9}$$

where, the juvenile population density is denoted by x , the adult population density by y , and the time delay is denoted by $(t - \tau)$. The growth coefficient α represents the rate at which juvenile grows, the maturation rate β the rate at which juvenile matures, the juvenile mortality rate δ_1 the rate at which juvenile die, and the adult mortality rate δ_2 the rate at which adult die. E is the amount of resources used for harvesting; m is the half-saturation constant for harvesting (density at which harvesting rate is half of the maximum), n is the conversion factor (relating harvesting rate to juvenile density), γ is the competition coefficient (the rate at which adult compete for resources), and h is the harvesting coefficient (the rate at which juveniles are harvested).

General Objectives

The study aimed to compare the dynamics of model (6) and model (9) and to assess the effect of time delay on the stage structure model with Michaelis Mentens-type harvesting.

Specific Objectives

The specific objectives of the study were:

1. to develop non-delay stage structured juvenile-adult model and then assess the stability using the coexisting equilibrium,
2. to develop a delay stage structured juvenile-adult model and then assess the stability using the coexisting equilibrium,
3. to incorporate the functional response in model developed in (1) and (2),
4. to prove the existence of all steady states of the system (9) and discuss their stability analysis, stability switch and Hopf bifurcation,
5. then use numerical simulation to compare the dynamics of new model (9) and the existing model (6).

Assumption of the Model

1. assume that the harvesting is moderate and well managed. Thus, not all juveniles are harvested or removed instantly (immediately).
2. Juveniles also contribute to adult populations.

Significant of the study

In the study and investigation of predator-prey modeling, mathematical modeling is essential. It helps us simulate various ecological processes, thus improving our understanding of their feeding patterns and mutualistic relationships. The field of predator-prey interactions has been the subject of extensive research, but there has not been much work done on mathematical models that examine how time delays affect stage structure models with Michaelis-Mentens-type harvesting. In order to avoid over-exploitation and depletion of ecological resources, this study will guarantee and regulate the appropriate management of harvesting rates. In addition, it will introduce an additional school of thought

that will help researchers comprehend the effects of delay disturbance on harvesting.

Delimitation

Finding the effects of time delay on the stage structure model with harvesting akin to Michaelis-Mentens is the only focus of this study. Not all of the ecosystem's effects were examined.

Limitation

This study examines how a time delay affects a stage structure model that uses harvesting of the Michaelis-Mentens type. While crucial, it is insufficient to address every issue pertaining to harvesting in the environment. For the ecosystem to grow and be sustainable, more work must be done to improve it.

Definition of Terms

- Definition 1 (Stability)

In a predator-prey system, stability is the propensity of both predator and prey populations to hold steady over time without undergoing dramatic fluctuations or collapses. A stable predator-prey system is characterized by a dynamic equilibrium in which the populations oscillate around a relatively constant mean abundance.(Beddington *et al.*,1976; Boyce, 2000)

- Definition 2 (Asymptotically Stable)

When populations of both the predator and prey species gradually approach and stay close to their equilibrium values, this sort of stability is known as asymptotic stability in a predator-prey system. This is (Mchich

et al., 2007). In other words, the predator and prey populations may fluctuate around their equilibrium abundances, but they eventually settle into a stable pattern of oscillation.

Mathematically, asymptotic stability is often characterized by solutions to the equations describing the predator-prey dynamics converging towards a stable equilibrium point, known as the steady-state or equilibrium solution. This means that if the system experiences small perturbations or disturbances, it will eventually return to its stable equilibrium state.

In a predator-prey system, asymptotic stability indicates that the populations of predators and prey interact in a way that allows them to co-exist over the long term without one species driving the other to extinction. Achieving asymptotic stability in such systems is often a desirable outcome, as it reflects a balanced and sustainable relationship between predator and prey populations. (Arumugam *et al.*, 2020).

- Definition 3 (Hopf Bifurcation)

Karaaslanlı (2012). A Hopf bifurcation is a type of local bifurcation that occurs when a continuous time system's focus, or fixed point, loses stability in response to a parameter variation. In other words, a Hopf bifurcation happens when a periodic solution or limit cycle that revolves around an equilibrium point appears or disappears as a parameter is changed.

- Definition 4 (Saddle node bifurcation)

In a saddle-node bifurcation, two fixed points of a dynamical system collide and annihilate one another locally. The most common use of saddle-node bifurcation is in the context of continuous dynamical systems. The same bifurcation is frequently referred to as a fold bifurcation in discrete dynamical systems. (Guo & Wu, 2013).

- Definition 5 (Functional Response)

The connection between a predator's rate of eating or consumption and the density of its prey is known as a "functional response" in ecology. It explains how variations in prey density affect a predator's feeding rate.(Fransz, 1974).

- Definition 6 (Stage Structure)

Refers to the division of a population into distinct stages or classes based on specific life history traits or characteristics. These stages often represent different developmental or reproductive phases in an organism's life cycle Cole (1954). Stage structure is particularly relevant in populations with complex life cycles, such as many plants, insects, and vertebrates, where individuals undergo distinct life stages (example, juvenile, adult) with different growth rates, reproductive capacities, and survival probabilities.

Understanding stage structure is essential for studying population dynamics as it affects vital rates such as birth rates, death rates, and growth rates. By modeling the dynamics of each stage within a population, researchers can gain insights into how changes in environmental conditions, demographic parameters, or management interventions impact population growth, persistence, and stability over time. This understanding is crucial for effective conservation and management of populations in natural ecosystems.

- Definition 7 (Stability switch)

The term "stability switch" describes an abrupt shift in a system's stability characteristics, which frequently happens when a parameter or variable surpasses a crucial value. This change can lead to a transition from

Stability to instability (or vice versa) and One type of stability to another (example, from asymptotic stability to oscillatory stability).

- Definition 8 (Positive steady state)

A positive steady state refers to a stable equilibrium point where the population sizes of all species or variables in the system are greater than zero. None of the species or variables in the system go extinct and the equilibrium point is stable.

Organization of the study

This thesis is organized and structured into five chapters. Chapter one talks about the meaning of harvesting and the groups we have in the ecosystem. Background of the study, the statement of the problem, the purpose of the problem, the research objectives, limitation and delimitation. Chapter two looks at related literature reviews of other research works. Chapter three provides an in-depth analysis of the effect of time delay on stage structure model with Michaelis-Mentens-type harvesting. Areas such stability analysis and Hopf bifurcation of the model were looked at. Numerical simulation and analysis were done at chapter four. We finally concluded the thesis with relevant recommendation in chapter five.

CHAPTER TWO

LITERATURE REVIEW

Introduction

In this section, a range of research on the predator-prey paradigm written by various academics are covered, which Lotka-Volterra initially proposed. The relationships within the ecosystem are examined by the different authors. The topics examined include existence, reproduction, and nutrition. As a result, the living organisms of the ecosystem continue to flourish and exist.

According to Andrews and McLone (1976), mathematical modeling is the representation of real-world issues using mathematical terminology and methods to better understand the importance and characteristics.

Following the definition, the utilization of empirically linked literature on the impacts of Michaelis-Mentens-Type harvesting on stage structure models with delays will be the main focus of this chapter.

Brief History on Model

According to Vaidyanathan (2016), the Lotka-Volterra model is a pair of first-order non-linear differential equations that describe the dynamics of a biological system involving two species. While one functions as a predator, the other as a victim. Over time, they interact, and the model has the following shape:

$$\begin{aligned}\frac{dx}{dt} &= \alpha x - \beta xy, \\ \frac{dy}{dt} &= \delta xy - \gamma y,\end{aligned}\tag{10}$$

where y and x denote the population densities of the predator and prey,

respectively, and t denotes time. The instantaneous growth rates of the two populations are represented by $\frac{dx}{dt}$ and $\frac{dy}{dt}$. The maximum prey per capita growth rate and the impact of predators on prey growth rate are represented by α and β , respectively. Additionally, the predator's per capita death rate and the impact of prey on its growth rate are described by γ and δ , respectively.

Scholars frequently use this model to examine how the ecological system's dynamics relate to mutualism, illnesses, competition, harvesting, and predator-prey relationships. Understanding the model requires an examination of the life stages of all living things. "Juvenile and adulthood" are the two life stages that every living thing or species experiences. We refer to this as stage-structure. The stage structure model illustrates real-world occurrences, notable variations, and traits of species during various life stages. Nonetheless, a number of academics have examined the stage structure model and have produced a number of outstanding outcomes regarding the model's extinction, persistence, and allure worldwide.

According to Lei (2018), considered a two species stage structure commensalism model:

$$\begin{aligned}\frac{dx_1}{dt} &= \alpha x_2 - \beta x_1 - \delta_1 x_1, \\ \frac{dx_2}{dt} &= \beta x_1 - \delta_1 x_2 - \gamma x_2^2 + dx_2 y, \\ \frac{dy}{dt} &= y(b_2 a_2 y),\end{aligned}\tag{11}$$

where the following positive constants are present: $\gamma, d, a_2, b_2, \beta, \delta_1, \delta_2$, and γ . At time t , the first species densities are represented by the juvenile and adult values, x_1 and x_2 , respectively; the second species is represented by y . A stability analysis was conducted on them. According to their research, one of the best strategies to stop the extinction of threat-

ened species in the environment is through high levels of inter-species cooperation.

Given that young animals require time to mature, the stage structure predator-prey model was presented by Ma *et al.* (2008), Chen *et al.* (2012), Chen, Chen, *et al.* (2013), and Wang *et al.* (2013). The primary model looks like this:

$$\begin{aligned}\frac{dx_1(t)}{dt} &= r_1(t)x_2(t) - d_{11}x_1(t) - r_1(t - \tau_1)e^{-d_{11}r_1}x_2(t - \tau_1), \\ \frac{dx_2(t)}{dt} &= r_1(t - \tau_1)e^{-d_{11}r_1}x_2(t - \tau) - d_{12}x_2(t) - b_1(t)x_2^2(t) - c_1(t)x_2(t)y_2(t), \\ \frac{dy_1(t)}{dt} &= r_2(t)y_2 - d_{22}y_1(t) - r_2(t - \tau_2)e^{-d_{22}r_2}y_2(t - \tau_2), \\ \frac{dy_2(t)}{dt} &= r_2(t - \tau_1)e^{-d_{22}r_2}y_2(t - \tau) - d_{21}y_2(t) - b_2(t)y_2^2(t) - c_2(t)y_2(t)x_2(t),\end{aligned}\tag{12}$$

where $x_1(t), x_2(t)$ represent, respectively, the juvenile and adult prey species densities at time t . At each time t , the juvenile and adult predator species densities are described by $y_1(t), y_2(t)$, respectively. Discussions were held over the model's stability, extinction, and persistence. The findings demonstrate that the system can persist under the right circumstances and that a predator's extinction does not always follow that of its prey population.

Scholars examined the many forms of harvesting and their effects on the ecology in order to guarantee the ecosystem's sustainable development and to optimize economic rewards.

May *et al.* (1979) proposed two methods of harvesting. *Linear harvesting* is proportionate to the number of harvested populations and is expressed as $h = qEx$. The constant *Constant harvesting* remains constant regardless of the quantity of populations that are harvested. When we harvest continuously, we are unable to gather a set number of species

annually.

Clark (1979) proposed a nonlinear harvesting method.

The expression $h = \frac{qEx}{(mE+nx)}$ can be used to represent nonlinear harvesting, commonly known as Michaelis-Menten-type harvesting. In the event that either $x \rightarrow \infty, h \rightarrow \frac{qE}{n}$ or $E \rightarrow \infty, h \rightarrow \frac{qx}{m}$; The harvesting model known as the Michaelis-Mentens type examines the viability of harvesting from both an economic and biological perspective.

Xiao and Lei (2018) investigated how harvesting affected the dynamics of a single species stage structure model. It is in the following form:

$$\begin{aligned}\frac{dx_1}{dt} &= \alpha x_2 - \beta x_1 - \delta_1 x_1 - q_1 E m x_1, \\ \frac{dx_2}{dt} &= \beta x_1 - \delta_2 x_2 - \gamma x_2^2 - q_2 E m x_2,\end{aligned}\tag{13}$$

where x_1, x_2 are the species densities of juveniles and adults at time t , respectively. The system has a boundary equilibrium that is globally asymptotically stable $E_0(0, 0)$, as demonstrated by the author, if $\alpha < (\delta_2 + q_2 E m)(1 + \frac{\delta_1 + q_1 E m}{\beta})$. A global asymptotically stable equilibrium of $A(x_1^*, x_2^*)$ for the system exists if and only if $\alpha > (\delta_2 + q_2 E m)(1 + \frac{\delta_1 + q_1 E m}{\beta})$. The system operates in a very basic manner because there are only two cases.

It is wise to take into account the impact of Michaelis-Menten-Type harvesting on dynamic behavior because it has a bigger effect on the model dynamics than linear harvesting does, making the model dynamics more complex, given that it depicts the harvesting procedures.

Liu *et al.* (2018), investigated how Michaelis-Menten-Type harvesting affects the dynamics of the amensalism model; the revised model looks

like this:

$$\begin{aligned}\frac{dx}{dt} &= a_2x - b_1x^2 - c_1(1-k)xy - \frac{qE(1-k)x}{m_1E + m_2(1-k)x}, \\ \frac{dy}{dt} &= a_2y - b_2y^2.\end{aligned}\quad (14)$$

The research demonstrated that, when specific criteria are met, the system exhibits saddle bifurcation and trans-critical bifurcation, from which they derive the highest sustainable harvest threshold.

In order to ascertain the predator-prey model's influence both historically and currently, numerous scholars additionally use time delay to the model.

Yan and Li (2006) added a time delay τ to the population densities of the predator-prey model. The model has this form:

$$\begin{aligned}\dot{x}(t) &= x(t) [r_1 - a_{11}x(t - \tau) - a_{12}y(t)], \\ \dot{y}(t) &= y(t) [-r_2 + a_{21}x(t) - a_{22}y(t - \tau)].\end{aligned}\quad (15)$$

The model looked into the Hopf bifurcation properties and system stability using the center manifold theorem and normal form theory.

Faria (2001), studied the stability and Hopf bifurcation of the predator-prey model with two unique delays. The framework is his role model:

$$\begin{aligned}\dot{x}(t) &= x(t) [r_1 - a_{11}x(t) - a_{12}y(t - \tau)], \\ \dot{y}(t) &= y(t) [-r_2 + a_{21}x(t - \tau) - a_{22}y(t - \tau)].\end{aligned}\quad (16)$$

The stability and Hopf bifurcation of the following delayed system were examined, taking into account the viewpoint of Kuang and Smith (1993) and Yan and Zhang (2008):

$$\begin{aligned}\dot{x}(t) &= x(t) [r_1 - a_{11}x(t - \tau) - a_{12}y(t - \tau)], \\ \dot{y}(t) &= y(t) [-r_2 + a_{21}x(t) - a_{22}y(t - \tau)].\end{aligned}\tag{17}$$

Based on system (15) to (17), Xu *et al.* (2011), introduced the model which have delay τ on each term. The model examined Hopf bifurcation analysis and stability for the two-delay Lotka-Volterra predator-prey model. This is how the model looks:

$$\begin{aligned}\dot{x}(t) &= x(t) [r_1 - a_{11}x(t - \tau_1) - a_{12}y(t - \tau_2)], \\ \dot{y}(t) &= y(t) [-r_2 + a_{21}x(t - \tau_2) - a_{22}y(t - \tau_1)],\end{aligned}\tag{18}$$

With variables $x(t)$ and $y(t)$, respectively, represent the population densities of the predator and prey at time t . $r_1 > 0$ indicates the intrinsic growth rate of prey, while r_2 indicates the death rate of predators. In the first equation of the system, τ_2 indicates the predator's hunting delay to prey; in the second equation, τ_2 indicates the predator's maturation delay. The parameters $a_{ij} = (i, j = 1, 2)$ are all positive constants. The prey's gestation period is represented by τ_1 .

The work of Yu *et al.* (2020) has greatly influenced our model as it studies the dynamics behaviors of a single species stage structure model with juvenile population harvesting in the Michaelis-Menten style. The form of the model was:

$$\begin{aligned}\frac{dx}{dt} &= \alpha y - \beta x - \delta_1 x - \frac{hEx}{mE + nx}, \\ \frac{dy}{dt} &= \beta x - \delta_2 y - \gamma y^2.\end{aligned}\tag{19}$$

The model was created to examine the effects of juvenile harvesting on the environment. According to their findings, harvesting of the Michaelis-Menten type is more susceptible to the effects of model dynamics.

The research showed that the model has extensive dynamical behaviors and a variety of positive stable states. The first bi-stability phenomenon states that the model is persistence if $b < c(e - a)$, $\Delta(b) < 0$, and the initial value is in the first quadrant. From a biological perspective, juvenile and adult species are capable of stable coexistence. The second bi-stability phenomena suggests that both species will coexist under certain circumstances and that both species will go extinct under other circumstances.

In other words, if the juvenile population's birth rate is low enough, the species will go extinct. If $e < a$, that is, $\alpha < \delta_2(\beta + \frac{\delta_1}{\beta})$, then the border equilibrium $E_0(0, 0)$ is globally asymptotically stable. Furthermore, studies demonstrate that the rate of species extinction is accelerated by ongoing and increased exploitation.

At $E_3(x_3, y_3)$, the system will have a unique globally asymptotically stable internal equilibrium if and only if $b > c(e - a)$ and $\Delta(b) > 0$. In other words, harvesting won't impact the model's persistence if certain requirements are satisfied. However, increasing harvesting will also result in lower species population densities.

Chapter Summary

This chapter examines the many perspectives held by academics regarding the Lotka-Volterra model. Their opinions and input improve our knowledge of the ecology. None of the mathematical models that we now have about existence, harvesting, and harvesting with Michaelis-Mentens-Type harvesting have been developed for the impacts of time delays on stage structured models. Decision-makers in the fisheries, wildlife management, and other ecological systems will therefore benefit from a combination of this work and those mentioned above. where appropriate har-

vesting techniques will be used to ensure the continued existence of the species.

CHAPTER THREE

RESEARCH METHODS

Introduction

The stability analysis, Hopf bifurcation, and presence of solution of the delayed stage-structured model with Michaelis-Mentens type harvesting are covered in this chapter. The current literature suggested by (Yu *et al.*,2020) served as the foundation for this study.

The existing model is of the form:

$$\begin{aligned}\frac{dx}{dt} &= \alpha y - \beta x - \delta_1 x - \frac{hEx}{mE + nx}, \\ \frac{dy}{dt} &= \beta x - \delta_2 y - \gamma y^2.\end{aligned}\tag{20}$$

Table 1: Parameters and their Description

Parameters	Descriptions
α	per capita birth rate of the juvenile population
β	surviving rate of the juvenile to reach adulthood
δ_1	death rate of the juvenile population
δ_2	death rate of adult population
γ	intraspecific competition of the adult population
h	catchability coefficient of the adult population
E	external effort devoted to the harvesting of the juvenile population

Source: Yu *et al.*(2020)

The model will be broken down into two forms: a delayed structure model with no functional response, where its dynamics will be examined, and a non-delayed stage structure model.

The non-delay stage structure model has the form:

$$\begin{aligned}\frac{dx}{dt} &= \alpha y - \beta x - \delta_1 x, \\ \frac{dy}{dt} &= \beta x - \delta_2 y - \gamma y^2.\end{aligned}\tag{21}$$

The form of the delayed structure model without functional response is:

$$\begin{aligned}\frac{dx}{dt} &= \alpha y - (\beta + \delta_1)x(t - \tau), \\ \frac{dy}{dt} &= \beta x - \delta_2 y - \gamma y^2.\end{aligned}\tag{22}$$

We make the following transformation on system(20) :

$$\bar{x} = \frac{\gamma}{\delta_1}x, \quad \bar{y} = \frac{\gamma}{\delta_2}y, \quad \bar{t} = \delta_2 t.$$

and by dropping the bars, the following system was obtained. (Yu *et al.*, 2020) .

$$\begin{aligned}\frac{dx}{dt} &= y - ax - \frac{bx}{c+x}, \\ \frac{dy}{dt} &= ex - y(1+y).\end{aligned}\tag{23}$$

Then the new model with delay on the juvenile term is of the form after transformation:

$$\begin{aligned}\frac{dx}{dt} &= y - ax(t - \tau) - \frac{bx}{c+x}, \\ \frac{dy}{dt} &= ex - y(1+y),\end{aligned}\tag{24}$$

where;

$$a = \frac{\beta + \delta_1}{\delta_2}, \quad b = \frac{hE\gamma}{\alpha\delta_2 n}, \quad c = \frac{mE\gamma}{n\alpha}, \quad e = \frac{\alpha\beta}{\delta_2^2}, \quad t = \tau t$$

with initial conditions:

$$x(t) = x_0 \geq 0, \quad y(t) = y_0 \geq 0, \quad t \in [-\tau, 0].\tag{25}$$

Stability Analysis

The qualitative behavior of the steady state of the system is examined. Stability analysis will be performed on systems (21) to (24).

Non-Delay Structure Model Without Harvesting

From system (21), the stability analysis is performed using the coexisting equilibrium $E_*(x_*, y_*)$;

At the equilibrium point, $\frac{dx}{dt} = 0$ and $\frac{dy}{dt} = 0$. Then

$$\begin{aligned}\alpha y - \beta x - \delta_1 x &= 0, \\ \beta x - \delta_2 y - \gamma y^2 &= 0.\end{aligned}\tag{26}$$

The coexisting equilibrium point of $E_*(x_*, y_*)$ will be,

$$x_* = \left(\frac{\alpha^2 \beta - \alpha \delta_2 (\beta + \delta_1)}{\gamma} \right), \quad \text{and} \quad y_* = \left(\frac{\alpha \beta - \delta_2 (\beta + \delta_1)}{\gamma (\beta + \delta_1)} \right).$$

The following regions may be obtained:

$$F_1 = (\delta_1, \beta, \gamma) = -\delta_1 \leq \beta \leq \delta_1,$$

$$F_2 = (\delta_1, \beta, \gamma) = \beta > -\delta_1,$$

$$F_3 = (\delta_1, \beta, \gamma) = -\delta_1 < \beta < \delta_1.$$

Results 1:

The equilibrium parameter E_* exist if $\beta > -\delta_1$, hence from the above, the equilibrium E_* has region F_2 and F_3 .

Theorem 1

If both eigenvalues have negative real parts, the coexisting equilibrium E_* is locally asymptotically stable; however, if at least one of the eigenvalues has a positive real component, the equilibrium is unstable.

The local stability can be ascertained by looking at the eigenvalue from the characteristic equation:

$$\det(\mathbf{J}_0 + \mathbf{J}_1 e^{-\lambda\tau} - \lambda\mathbf{I}) = 0. \quad (27)$$

Proof for $E_*(X_*, Y_*)$ where $\tau = 0$:

$$J(0) = \begin{bmatrix} -(\beta + \delta_1) & \alpha \\ \beta & -(\delta_2 + 2\gamma y_e) \end{bmatrix} \quad (28)$$

Substituting the matrices into the characteristics equation as;

$$= \det \left(\begin{bmatrix} -\beta - \delta & \alpha \\ \beta & -\delta_2 - 2y_e \end{bmatrix} - \lambda \begin{bmatrix} 1 & 0 \\ 0 & 1 \end{bmatrix} \right) \quad (29)$$

$$= \det \left(\begin{bmatrix} (-\beta - \delta) - \lambda & \alpha \\ \beta & -(\delta_2 - 2y_e) - \lambda \end{bmatrix} \right). \quad (30)$$

Expanding and rearranging:

$$\lambda^2 + (\beta + \delta_1 + \delta_2 + 2\gamma y_e)\lambda + (-\beta + \delta_1)(\delta_2 + 2\gamma y_e) - \alpha\beta = 0.$$

The characteristics equation of $J(E_*)$ is of the form;

$$\lambda^2 - A\lambda + B = 0, \quad (31)$$

solving for λ , we use the quadratic formula;

$$\lambda = \frac{-b \pm \sqrt{b^2 - 4ac}}{2a},$$

where :

$$A = (\beta + \delta_1 + \delta_2 + 2\gamma y_e), \tag{32}$$

$$B = (-\beta + \delta_1)(\delta_2 + 2\gamma y_e) - \alpha\beta,$$

and the real part of the eigenvalues are;

$$\lambda_{1,2} = -\frac{(\beta + \delta_1 + \delta_2 + 2\gamma y_e)}{2}.$$

Therefore, λ_1 and λ_2 have a negative real part as, $(-\frac{A}{2})$. Meaning, the system has a stabilizing effect, trying to bring the populations back to the equilibrium point. However, in ecological terms, the system returns to equilibrium after a small disturbance, indicating a stable coexistence between juvenile and adult populations. The system's equilibrium point is unstable if $(A > 4B)$ as well. The populations will either show exponential growth or decay, and the system will move away from the equilibrium point, suggesting that the populations of juvenile or adult will either collapse or proliferate uncontrollably.

Delay Structure Model Without Harvesting

Also, from system (22), the stability analysis is investigated using $E_*(X_*, Y_*)$ as follows;

when, $\frac{dx}{dt} = 0$ and $\frac{dy}{dt} = 0$. Then,

$$\begin{aligned}\alpha y - (\beta + \delta_1)x(t - \tau) &= 0, \\ \beta x - \delta_2 y - \gamma y^2 &= 0.\end{aligned}\tag{33}$$

At equilibrium point $E_*(x_*, y_*)$ will be in the form;

$$x_* = \left(\frac{\alpha^2 \beta - \alpha \delta_2 (\beta + \delta_1)}{\gamma} \right) \quad \text{and} \quad y_* = \left(\frac{\alpha \beta - \delta_2 (\beta + \delta_1)}{\gamma (\beta + \delta_1)} \right)$$

Theorem 2

If the eigenvalues have a negative real portion, then the coexisting equilibrium E_* is locally asymptotically stable.

Proof

At every equilibrium (x_*, y_*) , the local stability will be ascertained by examining the eigenvalues from the characteristics equation. This can be achieved as follows:

$$\det(\mathbf{J}_0 + \mathbf{J}_\tau e^{-\lambda\tau} - \lambda \mathbf{I}) = 0.\tag{34}$$

At equilibrium, the Jacobian matrix is provided by:

$$J(E_0) = \begin{bmatrix} 0 & \alpha \\ \beta & -(\delta_2 + 2\gamma y_e) \end{bmatrix}\tag{35}$$

Moreover, the time delay's Jacobian matrix has the following form:

$$J_\tau = \begin{bmatrix} -(\beta + \delta_1) & 0 \\ 0 & 0 \end{bmatrix}\tag{36}$$

Substituting into system (34), we have:

$$= \det \left(\begin{array}{cc} \left[\begin{array}{cc} 0 & \alpha \\ \beta & -\delta_2 - 2\gamma_e \end{array} \right] + e^{-\lambda\tau} \left[\begin{array}{cc} -(\beta + \delta_1) & 0 \\ 0 & 0 \end{array} \right] & -\lambda \left[\begin{array}{cc} 1 & 0 \\ 0 & 1 \end{array} \right] \end{array} \right) \quad (37)$$

If $\tau = 0$, the matrix function simplifies to:

$$\left[\begin{array}{cc} -(\beta + \delta_1) - \lambda & \alpha \\ \beta & -(\delta_2 + 2\gamma_e) - \lambda \end{array} \right]$$

Solving the characteristic equation yields the eigenvalues:

$$\det \left(\left[\begin{array}{cc} -(\beta + \delta_1) - \lambda & \alpha \\ \beta & -(\delta_2 + 2\gamma_e) - \lambda \end{array} \right] \right) = 0$$

Expanding the determinant, we get:

$$[(-(\beta + \delta_1) - \lambda)(-(\delta_2 + 2\gamma_e) - \lambda) - \alpha\beta = 0]$$

Simplifying, we get:

$$\lambda^2 + (\beta + \delta_1 + \delta_2 + 2\gamma_e)\lambda + (\beta + \delta_1)(\delta_2 + 2\gamma_e) - \alpha\beta = 0$$

This means that, in the absence of delay, the characteristics equation will be in quadratic form at the coexisting equilibrium E_* :

$$\lambda^2 + A\lambda + B = 0 \quad (38)$$

where the coefficient of the constant are;

$$A = (\beta + \delta_1 + \delta_2 + 2\gamma y_e),$$

$$B = (\beta + \delta_1)(\delta_2 + 2\gamma y_e) - \alpha\beta,$$

hence we will have

$$\lambda_{1,2} = \frac{-A \pm \sqrt{A^2 - 4B}}{2}$$

.

Since $\lambda_{1,2}$ of system (38), have negative real part $-\frac{A}{2} < 0$, consequently, for $\tau = 0$, E_* is locally asymptotically stable.

According to system (37), if $\tau \neq 0$, the matrix will have the following form:

$$\det \left(\begin{bmatrix} -e^{-\lambda\tau}(\beta + \delta_1) - \lambda & \alpha \\ \beta & -(\delta_2 + 2\gamma y_e) - \lambda \end{bmatrix} \right) = 0,$$

let, $a_2 = (\delta_2 + 2\gamma y_e)$, $b_1 = (\beta + \delta_1)$, $e = \alpha\beta$,

then substituting and expanding,

$$(b_1 e^{-\lambda\tau} + \lambda)(a_2 + \lambda) - e = 0,$$

the characteristics equation will be in the form

$$\lambda^2 + a_2\lambda + b_1\lambda e^{-\lambda\tau} + a_2b_1e^{-\lambda\tau} - e = 0 \quad (39)$$

If the time delay alters the stability behavior, System (39) needs a root $\lambda = i\omega$ ($\omega > 0$) for a certain critical value of τ . Using system (3.21) and setting $\lambda = i\omega$, we have:

$$(i\omega)^2 + a_2(i\omega) + b_1(i\omega)e^{-(i\omega)\tau} + a_2b_1e^{-(i\omega)\tau} - e = 0,$$

using $e^{-i\omega} = \cos(\omega) + isin(\omega)$ taking the real and imaginary components, simplifying, and substituting in the above, we have,

$$\begin{aligned} -\omega^2 - b_1\omega sin(\omega\tau) + a_2b_1cos(\omega\tau) - e &= 0, \\ a_2\omega + b_1cos(\omega\tau) + a_2b_1sin(\omega\tau) &= 0, \end{aligned} \quad (40)$$

squaring each term and adding results in system (39) gives,

$$\begin{aligned} \omega^4 + a_2^2\omega^2 - b_2^2\omega^2 + a_2b_1^2 - e^2 &= 0, \\ \omega^4 + (a_2^2 - b_2^2)\omega^2 + a_2b_1^2 - e^2 &= 0. \end{aligned} \quad (41)$$

Let $\rho = \omega^2$, $A = (a_2^2 - b_2^2)$, and $B = (a_2b_1^2 - e^2)$,

then we will have the quadratic function:

$$\rho^2 + A\rho + B = 0,$$

using the quadratic formula, we will have;

$$\rho = \frac{-A \pm \sqrt{A^2 - 4B}}{2},$$

It follows that the coexisting equilibrium E_* is asymptotically stable for $\tau \neq 0$ since the real portion $-\frac{A}{2}$ is negative.

Delayed Functional Response Model

At equilibrium, when $\frac{dx}{dt} = 0$ and $\frac{dy}{dt} = 0$, then system (24) will be in the form:

$$\begin{aligned} y_* - ax_*(t - \tau) - \frac{bx_*}{c + x_*} &= 0, \\ ex_* - y_*(1 + y_*) &= 0, \end{aligned} \quad (42)$$

the system (24) possess three forms of equilibria, thus;

- (i) the trivial equation $E_0(0, 0)$,
- (ii) the juvenile only equilibrium $E_1(1, 0)$, and
- (iii) the coexisting equilibrium $E_*(x_*, y_*)$. Thus from system (42),

$$y_* = ax_* + \frac{bx_*}{c + x_*}, \quad (43)$$

and x_* satisfies

$$p_3x_*^3 + p_2x_*^2 + p_1x_* + p_0 = 0, \quad (44)$$

where,

$$\begin{aligned} p_0 &= [c(ce - b) - a^2], \quad p_1 = [2ec - a(ac^2 + 2) - b(2c + b)], \\ p_2 &= [e - b - a(2ac - 1)], \quad p_3 = -a^2. \end{aligned}$$

The trivial equation E_0 is saddle and juvenile equilibrium E_1 is asymptotically stable as they exist. However, the coexisting equilibrium either $b < ce$ with $c < x_* < \frac{1}{2}a$ or $b \geq ce$ with $0 < x_* < 1$, then we have the coexisting equilibrium to be:

$$x_* = \frac{(2a^2c + a + b - e) \pm \sqrt{(e - a - b - 2a^2c)^2 + 4a^2(2ec - 2bc - 2a - a^2b^2 - b^2)}}{2a^2}. \quad (45)$$

$$y_* = ax_* + \frac{bx_*}{c + x_*}. \quad (46)$$

Using the characteristic equation at an arbitrary equilibrium (x_e, y_e) , the eigenvalues will be analyzed to derive the local stability, which may be

found as:

$$\det(\mathbf{J}_0 + \mathbf{J}_\tau e^{-\lambda\tau} - \lambda\mathbf{I}) = 0, \quad (47)$$

where,

$$J_0 = \begin{bmatrix} -\frac{bc}{(c+x_e)^2} & 1 \\ e & -1 - 2y_e \end{bmatrix} \quad (48)$$

at an arbitrary equilibrium (x_e, y_e) ,

$$J_\tau = \begin{bmatrix} -a & 0 \\ 0 & 0 \end{bmatrix} \quad (49)$$

Stability Analysis when $\tau = 0$

. Theorem 3

Without delay harvesting ($\tau = 0, a \neq 0$) and placing system (48) and (49) into system (47), we obtain:

$$= \det \left(\begin{bmatrix} -\frac{bc}{(c+x_e)^2} & 1 \\ e & -1 - 2y_e \end{bmatrix} + e^{-\lambda\tau} \begin{bmatrix} -\alpha & 0 \\ 0 & 0 \end{bmatrix} - \lambda \begin{bmatrix} 1 & 0 \\ 0 & 1 \end{bmatrix} \right) \quad (50)$$

$$\det \left(\begin{bmatrix} -\left(\frac{bc}{(c+x_e)^2} + \alpha\right) - \lambda & 1 \\ e & -(1 + 2y_e) - \lambda \end{bmatrix} \right) = 0$$

Let $\frac{bc}{(c+x_e)^2} = a_1$. Then we will have,

$$\det \left(\begin{bmatrix} -(a_1 + \alpha + \lambda) & 1 \\ e & -(1 + 2y_e) - \lambda \end{bmatrix} \right) = 0,$$

$$(-(a_1 + \alpha + \lambda))(-(1 + 2y_e) - \lambda) - e(1) = 0,$$

Simplifying and rearranging, we get:

$$\lambda^2 + (a_1 + \alpha + 1 + 2y_e)\lambda + (a_1 + \alpha)(1 + 2y_e) - e = 0.$$

We can solve for λ using the quadratic formula:

$$\lambda = \frac{-\kappa \pm \sqrt{\kappa^2 - 4\eta}}{2},$$

where:

$$\kappa = (a_1 + \alpha + 1 + 2y_e),$$

$$\eta = ((a_1 + \alpha)(1 + 2y_e) - e),$$

As a result, the real component of each of the roots of (47) is negative.

Consequently, E_* is asymptotically stable.

Stability Analysis when $\tau \neq 0$

Let us now investigate the dynamics of the delayed system by analyzing how τ affects the coexisting equilibrium E_* 's stability.

Its Jacobian matrix is in the form;

$$= \det \left(\begin{array}{cc} \left[\begin{array}{cc} -\frac{bc}{(c+x_e)^2} & 1 \\ e & -1-2y_e \end{array} \right] + e^{-\lambda\tau} \begin{array}{cc} -\alpha & 0 \\ 0 & 0 \end{array} & -\lambda \begin{array}{cc} 1 & 0 \\ 0 & 1 \end{array} \end{array} \right) \quad (51)$$

$$\det \left(\begin{array}{cc} -\left(\frac{bc}{(c+x_e)^2} + \alpha e^{-\lambda\tau}\right) - \lambda & 1 \\ e & -(1+2y_e) - \lambda \end{array} \right) = 0,$$

$$\left(\frac{bc}{(c+x_e)^2} + \alpha e^{-\lambda\tau} + \lambda \right) (1+2y_e + \lambda) - e = 0,$$

$$(a_1 + \alpha e^{-\lambda\tau} + \lambda)(a_2 + \lambda) - e = 0,$$

$$a_1 a_2 + a_1 \lambda + a_2 \alpha e^{-\lambda\tau} + \lambda \alpha e^{-\lambda\tau} + a_2 \lambda + \lambda^2 - e = 0.$$

The properties of system (47)'s Jacobian matrix are provided by:

$$\lambda^2 + (a_1 + a_2)\lambda + \lambda \alpha e^{-\lambda\tau} + a_2 \alpha e^{-\lambda\tau} + a_1 a_2 - e = 0, \quad (52)$$

where

$$\left. \begin{array}{l} a_1 = \left[\frac{bc}{(c+x_e)^2} \right] \\ a_2 = (1+2y_e) \\ c = (a_1 a_2 - e) \\ k = a_2 \alpha \\ a = (a_1 + a_2) \\ h = \alpha \end{array} \right\} \quad (53)$$

Then we may have,

$$\lambda^2 + a\lambda + ke^{-\lambda\tau} + h\lambda e^{-\lambda\tau} - c = 0. \quad (54)$$

When there is no delay, E_* , the equilibrium, is stable. However, for some values of τ , a stability change may occur as a result of the delay's inclusion. Therefore, if delay-induced instability occurs at E_* , it will manifest itself as a Hopf bifurcation, which is defined as the occurrence of two or more purely imaginary eigenvalues, at the point at which τ reaches a critical value. Then, let $\lambda = i\omega$ ($\omega > 0$) be the root of the system (54) for some positive real ω in order for E_* to experience any stability change as a result of τ . When we enter $\lambda = i\omega$ into equation (54), we obtain:

$$(i\omega)^2 + a(i\omega) + ke^{-(i\omega)\tau} + h(i\omega)e^{-(i\omega)\tau} - c = 0,$$

using, $e^{-i\omega} = \text{Cos}(\omega) + i\text{Sin}(\omega)$,

hence, substituting and simplifying, real and imaginary part, we have:

$$-\omega^2 + k\cos(\omega\tau) - h\omega\sin(\omega\tau) - c = 0, \quad (55)$$

and

$$a\omega + k\sin(\omega\tau) + h\omega\cos(\omega\tau) = 0, \quad (56)$$

squaring each term and adding results in systems (55) and (56) gives:

$$\omega^4 + (a^2 - h^2)\omega^2 + (c^2 - k^2) = 0, \quad (57)$$

then the possible values of ω are :

$$\omega_{\pm} = \frac{1}{\sqrt{2}} \sqrt{(h^2 - a^2) \pm \sqrt{\Delta}}, \quad (58)$$

where

$$\Delta := \sqrt{(a^2 - h^2)^2 - 4\sqrt{(c^2 - k^2)}},$$

Let us determine the critical τ value that corresponds to a positive ω .

After system (55) and (56) are solved, we obtain:

$$\cos(\omega\tau) = \frac{ah\omega^2 + k\omega^2 + kc}{k^2 - h^2\omega^2} =: C(\omega), \quad (59)$$

$$\sin(\omega\tau) = \frac{(\omega^2 + c)(k^2 - h^2\omega) - k(ah\omega^2 + k\omega^2 + kc)}{(k^2h\omega - h^3\omega^3)} =: S(\omega). \quad (60)$$

Considering several cases pertaining to the existence of positive ω , we now examine the following categorization based on system (54).

Case I: No real ω exists

if at least one of the model (54)'s conditions can be met:

$$C_1 : (a^2 - h^2)^2 < 4\sqrt{(c^2 - k^2)},$$

$$C_2 : (h^2 - a^2) < 0 \quad \text{and} \quad (c^2 - k^2) > 0,$$

holds, then system (58) yield no positive result, consequently, the stability of the interior equilibrium E_* is unaffected by the delay.

Case II: Existence of only one positive ω :

This occurs when the following condition is met by the parameters:

$$C_3; (c^2 - k^2) < 0,$$

The ω_+ value is provided by,

$$\omega_+ = \frac{1}{\sqrt{2}} \sqrt{(h^2 - a^2) + \sqrt{\Delta}},$$

subsequently τ 's matching threshold values are,

$$\tau_n^+ = \begin{cases} \frac{\theta_+}{\omega_+} + \frac{2\pi n}{\omega_+} & \text{if } S(\omega_+) > 0, \\ \frac{2\pi - \theta_+}{\omega_+} + \frac{2\pi n}{\omega_+} & \text{if } S(\omega_+) < 0, \end{cases} \quad (61)$$

where

$$\theta_+ = \cos^{-1}\left(-\frac{a}{h}\right), \quad \theta_+ \in \left(0, \frac{\pi}{2}\right) \cup \left(0, \frac{3\pi}{2}\right), \quad n = 0, 1, 2, 3, \dots$$

Case III: Existence of two distinct positive of ω :

This is possible if these condition hold,

$$C_4; (a^2 - h^2) > 0,$$

$$(c^2 - k^2) > 0,$$

and

$$\sqrt{\Delta} > 0$$

then, will have two distinct positive ω_{\pm} ($\omega_+ > \omega_-$) is given by

$$\omega_{\pm} = \frac{1}{\sqrt{2}} \sqrt{(h^2 - a^2) \pm \sqrt{\Delta}}, \quad (62)$$

For the roots $\lambda = i\omega_{\pm}$ of system (52) to exist, the associated critical threshold value of τ_n^{\pm} of τ is shown to be:

$$\tau_n^+ = \begin{cases} \frac{\theta_+}{\omega_+} + \frac{2\pi n}{\omega_+} & \text{if } S(\omega_+) > 0, \\ \frac{2\pi - \theta_+}{\omega_+} + \frac{2\pi n}{\omega_+} & \text{if } S(\omega_+) < 0, \end{cases} \quad (63)$$

and

$$\tau_n^- = \begin{cases} \frac{\theta_-}{\omega_-} + \frac{2\pi n}{\omega_-} & \text{if } S(\omega_-) > 0, \\ \frac{2\pi - \theta_-}{\omega_-} + \frac{2\pi n}{\omega_-} & \text{if } S(\omega_-) < 0, \end{cases} \quad (64)$$

for $n = 0, 1, 2, 3, \dots$, where

$$\theta_{\pm} = \cos^{-1}\left(-\frac{a}{h}\right), \quad \theta_{\pm} \in \left(0, \frac{\pi}{2}\right) \cup \left(\frac{\pi}{2}, \pi\right), \quad (65)$$

Remarks 1;

If $\tau = \tau_n^{\pm}$, then the characteristics equation yield two distinct positive ω .

We differentiate (52) in respect to λ ;

proof;

$$F(\lambda, \tau) = \lambda^2 + (a_1 + a_2)\lambda + \lambda\alpha e^{-\lambda\tau} + a_2\alpha e^{-\lambda\tau} + a_1a_2 - e, \quad (66)$$

solving each terms individually and simplifying, we get;

$$\begin{aligned} \frac{dF}{d\lambda} &= 2\lambda + (a_1 + a_2) + \alpha e^{-\lambda\tau} - \alpha\lambda\tau e^{-\lambda\tau} - a_2\alpha\tau e^{-\lambda\tau}, \\ \frac{dF}{d\lambda} &= 2\lambda + (a_1 + a_2) + \alpha e^{-\lambda\tau} - \alpha\tau e^{-\lambda\tau}(\lambda + a_2) \end{aligned} \quad (67)$$

If $F(\lambda, \tau) = 0$, then,

$$\frac{dF}{d\lambda} = 0 \Rightarrow 2\lambda + (a_1 + a_2) + \alpha e^{-\lambda\tau} - \alpha\tau e^{-\lambda\tau}(\lambda + a_2). \quad (68)$$

Now, we look for the transversality criterion to identify the shift in stability across the threshold.

From (68),

$$2\lambda + (a_1 + a_2) + \alpha e^{-\lambda\tau} - \alpha\tau e^{-\lambda\tau}(\lambda + a_2) = 0,$$

$$e^{\lambda\tau} = \frac{\alpha - \alpha\tau(\lambda + a_2)}{-2\lambda - (a_1 + a_2)}, \quad (69)$$

After differentiating system (52) with regard to τ and assuming $\lambda \equiv \lambda(\tau)$, we have,

$$\left(\frac{d\lambda}{d\tau}\right)^{-1} = -\frac{-2\lambda - (a_1 + a_2)}{\lambda[\lambda^2 + (a_1 + a_2)\lambda + a_1a_2 - e]} + \frac{1}{\lambda[\lambda + a_2]} - \frac{\tau}{\lambda}, \quad (70)$$

$$\text{sign}\left(\text{Re}\left(\frac{d\lambda}{d\tau}\right)^{-1}\right)\Big|_{\tau=\tau_n^\pm} = \text{sign}\left(\text{Re}\left[\frac{-2\lambda - (a_1 + a_2)}{\lambda[\lambda^2 + (a_1 + a_2)\lambda + a_1a_2 - e]} + \frac{1}{\lambda[\lambda + a_2]}\right]\Big|_{\lambda=i\omega^\pm}\right)$$

$$= \text{sign}\left(\omega^4 - (a_1a_2 - e)^2 + 2a_2^2(\omega^2 - (a_1a_2 - e)) + a_2^2(a_1 + a_2)^2\Big|_{\omega=\omega^\pm}\right),$$

using system (57), we can prove that,

$$\omega^4 - (a_1a_2 - e)^2 + 2a_2^2(\omega^2 - (a_1a_2 - e)) + a_2^2(a_1 + a_2)^2,$$

$$= (2\omega^2 + (a^2 - h^2))(\omega^2 + a_2^2).$$

Hence using system (62),

$$\text{sign}\left(\text{Re}\left(\frac{d\lambda}{d\tau}\right)^{-1}\right)\Big|_{\tau=\tau_n^\pm} = \text{sign}(2\omega_\pm^2 + (a^2 - h^2))\Big|_{\omega=\omega^\pm}, \quad (71)$$

$$= \text{sign}(\pm\sqrt{\Delta}). \quad (72)$$

Therefore we must have,

$$\frac{d(\operatorname{Re}\lambda)}{d\tau}\Big|_{\tau=\tau_n^+} > 0 \quad \text{and} \quad \frac{d(\operatorname{Re}\lambda)}{d\tau}\Big|_{\tau=\tau_n^-} < 0,$$

provided $\Delta \neq 0$. Therefore, in this scenario, when $\tau = \tau_n^\pm$ and $\Delta \neq 0$, the transversality requirement is met.

Cooke and Grossman (1982), states that when the root $\lambda = i\omega_\pm$ of system (22) exists, it is evident that it is simple. Because of this, as the parameter τ grows through τ_n^+ (resp. τ_n^-), only one pair of conjugate complex eigenvalues will cross the imaginary axis C^0 from C^- to C^+ (resp. from C^+ to C^-). Therefore, when τ reaches the critical thresholds τ_n^\pm , the system (24) shows Hopf bifurcations around E_* .

Case IV: Existence of a two-fold positive ω .

If the subsequent condition is met, there are two-fold real positive ω .

$$C_5; \quad a^2 - h^2 > 0,$$

and $\Delta = 0$ is met, we have the following:

$$\omega_\pm = \frac{1}{\sqrt{2}} \sqrt{(a^2 - h^2)} = \omega_0(\text{say}),$$

and τ 's critical thresholds are provided by,

$$\tau_n^0 = \begin{cases} \frac{\theta_+}{\omega_0} + \frac{2\pi n}{\omega_0} & \text{if } S(\omega_0) > 0, \\ \frac{2\pi - \theta_+}{\omega_0} + \frac{2\pi n}{\omega_0} & \text{if } S(\omega_0) < 0, \end{cases} \quad (73)$$

where $n = 0, 1, 2, 3, \dots$, and

$$\theta_0 = \cos^{-1}\left(-\frac{a}{h}\right), \theta_0 \in \left(0, \frac{\pi}{2}\right) \cup \left(\frac{\pi}{2}, \pi\right), \quad (74)$$

from system (70),

$$\left(\frac{d\lambda}{d\tau}\right)^{-1} \Big|_{\tau=\tau_n^0} = \frac{-2i\omega_0 - (a_1 + a_2)}{\omega_0[(a_1 + a_2)\omega_0 + i(a_1a_2 - e - \omega_0^2)]} + \frac{1}{\omega_0[\omega_0 + ia_2]} - \frac{\tau_n^0}{i\omega_0}, \quad (75)$$

$$= i\frac{\Gamma}{\omega_0},$$

where,

$$\Gamma = \frac{a_2}{\omega_0^2 + a_2^2} - \frac{(a_1 + a_2)(a_1a_2 - e + \omega_0^2)}{(a_1 + a_2)^2\omega_0^2 + (a_1a_2 - e - \omega_0^2)^2} + \tau_n^0.$$

Therefore,

$$\frac{d(Re\lambda)}{d\tau} \Big|_{\tau=\tau_n^0} = 0,$$

Considering $\Gamma \neq 0$, $\tau = \tau_n^0$ violates the transversality restriction. For $\tau = \tau_n^0$, the Hopf bifurcations are degenerate.

Pati and Ghosh (2022) examined the dynamics around the critical thresholds of τ in a predator-prey system with delayed carrying capacity, considering a degenerate scenario. When τ exceeds the thresholds, they showed the existence of both sub- and super-critical limit cycles and that the system is stable with respect to τ outside of the thresholds. So far, we have identified the critical threshold time delays for system (24) and developed various parametric requirements for the occurrence of Hopf bifurcations near equilibrium E_* . In order to understand the stability alteration of E_* depending on ω and the distribution of the time delay thresholds $\tau = \tau_n^\pm$, we provide some results below.

Remarks II.

The characteristics equation (22) does not have a completely imaginary eigenvalue $\lambda = i\omega$ when there is no positive ω and at least one of the

conditions C_1 and C_2 given in the **Case I** is satisfied. Stated otherwise, the eigenvalues are non-crossing of the imaginary axis C^0 . As such, the stability of the equilibrium E_* with regard to τ remains unchanged.

Remarks III.

When E_* is locally stable for $\tau = 0$, then

(i) if C_3 in the **Case II** holds, then when τ crosses the threshold τ_0^+ , the equilibrium E_* becomes unstable. In other words, E_* is unstable for all $\tau > \tau_0^+$ and locally stable for $\tau \in [0, \tau_0^+)$.

(ii) The same phenomenon as in (i) will occur if the condition C_4 in the **Case III** holds, and $\tau_0^+ < \tau_1^+ < \tau_0^-$. Specifically, E_* is locally stable for $\tau \in [0, \tau_0^+)$ and unstable for $\tau > \tau_0^+$. In this case, the coexisting equilibrium E_* has a stability change.

(iii) if C_4 holds and $0 < \tau_0^+ < \tau_0^- < \tau_1^+ < \tau_1^- \dots < \tau_k^+ < \tau_{k+1}^+ < \tau_k^- < \dots$ for some positive integer K . Then the equilibrium E_* is locally asymptotically stable for $\tau \in [0, \tau_0^+)U(\tau_0^-, \tau_1^+)U\dots U(\tau_{k-i}^-, \tau_1^+)$. E_* is unstable for $\tau \in (\tau_0^+, \tau_0^-)U(\tau_1^+, \tau_0^-)U\dots U(\tau_{k-1}^+, \tau_{k-1}^-)U(\tau_k^+, \infty)$ and the system undergoes Hopf bifurcations around E_* for $\tau = \tau_j^{pm}, \tau_K^+, j = 0, 1, 2, \dots, K - 1$. Consequently, E_* experiences K switches from stable to unstable to stable with increasing τ .

Remarks IV.

When E_* is locally unstable for $\tau = 0$, then,

(i) if the condition C_3 in the **Case II** holds, then E_* does not change its stability with respect to τ .

(ii) if the condition C_4 in **Case III** are met, and either $0 < \tau_0^+ < \tau_0^- < \tau_1^+ < \tau_1^- \dots$ or $0 < \tau_0^+ < \tau_1^+ < \tau_1^- < \dots$ holds, then no change of stability will occur at E_* with respect to τ .

(iii) if the condition C_5 in **Case IV** holds and $0 < \tau_0^- < \tau_0^+ < \tau_1^- < \tau_1^+ \dots <$

$\tau_-^1 < \tau_k^+ < \tau_{k+1}^+ < \dots$ for some positive integer K then the equilibrium E_* is unstable for all $\tau \in [0, \tau_0^-) \cup (\tau_0^+, \tau_0^-) \cup (\tau_1^+, \tau_2^-) \cup \dots \cup (\tau_{k-1}^+, \tau_k^-) \cup (\tau_k^+, \infty)$, then the equilibrium E_* is locally asymptotically stable for $\tau \in (\tau_0^+, \tau_0^-) \cup (\tau_1^+, \tau_1^-) \cup \dots \cup (\tau_k^+, \tau_k^-)$. So then equilibrium E_* will experience **k-unstability switches** from unstable \rightarrow stable \rightarrow unstable around the equilibrium E_* with increasing τ . The equilibrium remains unstable when $\tau > \tau_k^+$.

Remarks V

When $\tau = 0$, the equilibrium E_* is saddle, meaning that the delay has no bearing on the system's stability characteristics.

Chapter Summary

This chapter examined stability analysis, Hopf bifurcation, and the possibility of a solution to the impacts of time delay on the Michaelis-Mentens-type harvesting stage-structure model. The current study was informed by the existing literature, as suggested by (Yu *et al.*, 2020). A delay-structured model without a functional response and a non-delay-structured model were the two versions of model (6). When both eigenvalues are negative, both models are considered asymptotically stable. The model (6) is asymptotically stable at E_1 , and saddle at E_0 . After applying a time delay of $\tau \neq 0$, at E_* , the stability characteristics of the system change, leading to a stability switch. It resulted in oscillations and bifurcations and other behavioral changes in the system.

CHAPTER FOUR

RESULTS AND DISCUSSIONS

Introduction

The impacts of time delay on the stage structure model on the functional response that is, Michaelis-Mentens type harvesting was examined in this chapter. Coexisting equilibrium points of systems (21), (22), to (24) were simulated.

With the exception of time delay ($t - \tau$) in system (22), systems (21) and (22) will contain the identical table of variables and related values. A phase portrait comparison would be made between system (24), where $\tau = 0.2, 0.8$, and system (23), as previously worked on by (Yu *et al.*, 2020).

Numerical and Hopf-Bifurcation Analysis

A non-linear ordinary differential equation representing a functional response model with delay is numerically analyzed and presented. By adjusting the time delay, we begin with system (21) and move on to system (22) in order to examine the impacts that are produced in the figures that are explained.

System (23) is compared, and the research indicates that nonlinear harvesting can lead to a more complicated system dynamics than linear harvesting; for instance, the system admit the bistable stability attribute to (Yu *et al.*, 2020).

Also, system (24) examines how temporal delays affect the statements made on system (23).

Below is a presentation of the parameters and their values.

Table 2 : Parameters and their Values

Parameters	Descriptions	Values	Source
α	per capita birth rate of the juvenile population	1	(Yu <i>et al.</i> , 2020)
β	surviving rate of the juvenile population	0.75	(Yu <i>et al.</i> , 2020)
δ_1	dearth rate of the juvenile population	0.26	(Yu <i>et al.</i> , 2020)
δ_2	dearth rate of the adult population	0.25	(Yu <i>et al.</i> , 2020)
γ	intraspecific competition of the adult population	4	(Yu <i>et al.</i> , 2020)

Source: Yu *et al.*(2020)

The coexisting equilibrium for system (21) is

$$E_* = \left[\frac{(1)^2(0.75) - 1(0.25)(0.75+0.26)}{4}, \frac{1(0.75) - 0.25(0.75+0.26)}{4(0.75+0.26)} \right] = (0.1244, 0.1231).$$

As a result, neither the juvenile nor the adult will go extinct; instead, as a result, the beneficial actions of both species maintain the system's stability rather than making it unstable. The simulation of it is shown below. This is seen in Figures 1 and 2.

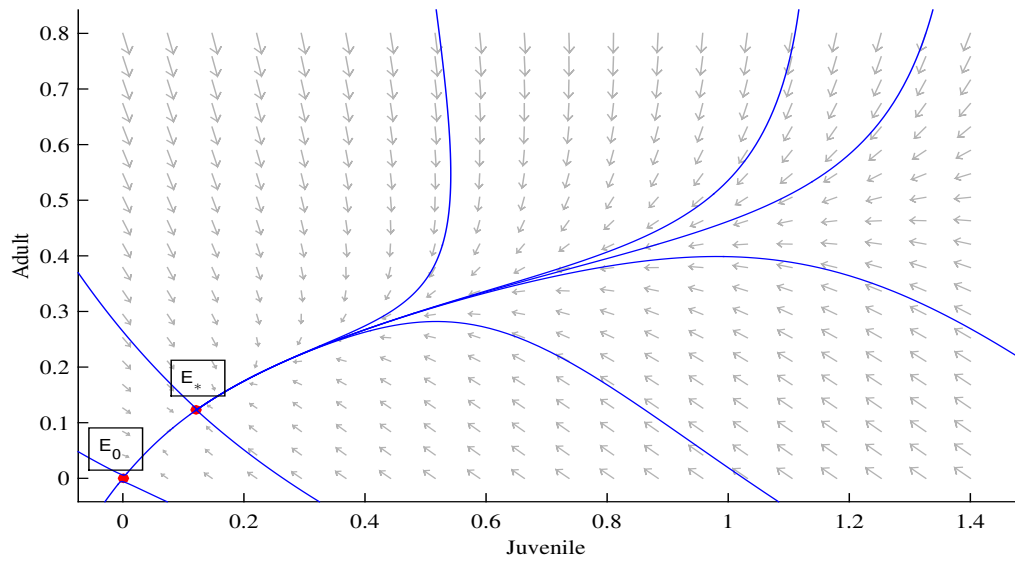


Figure 1: Phase portrait of model (21), $\alpha = 1, \beta = 0.75, \delta_1 = 0.26, \delta_2 = 0.25, \gamma = 4$.

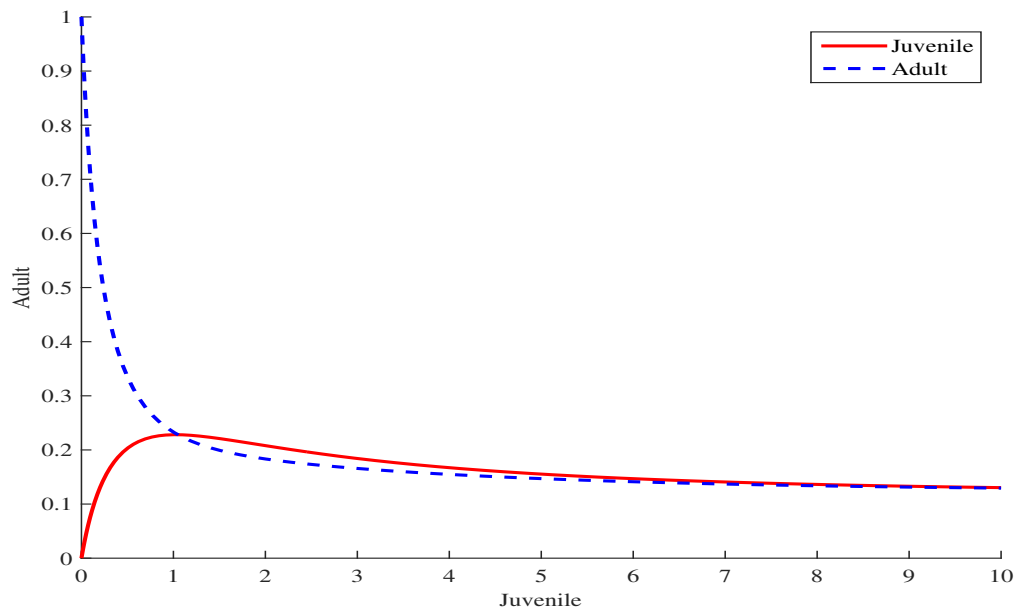


Figure 2: Simulation of model (21), $\alpha = 1, \beta = 0.75, \delta_1 = 0.26, \delta_2 = 0.25, \gamma = 4$.

Because E_0 is saddle, as seen in system (21) of Figure 2, which depicts a transient equilibrium between juvenile-adult, tiny adjustments can have a big impact on the populations and their interactions. When the juvenile population falls, it has a replica effect on the adult population. However, the presence of a nodal sink at E_* results in a steady and predictable juvenile-adult system, suggesting unstable population dynamics, which could lead to extinction of both species.

Given that system (21) and system (22) share the same coexisting equilibrium, the simulation indicates that the rate of growth of the adult rises with the amount of available juvenile. As a result, none of the species go extinct and the juvenile population increases with little affect on growth. The next Figure 3 and 4 demonstrate this.

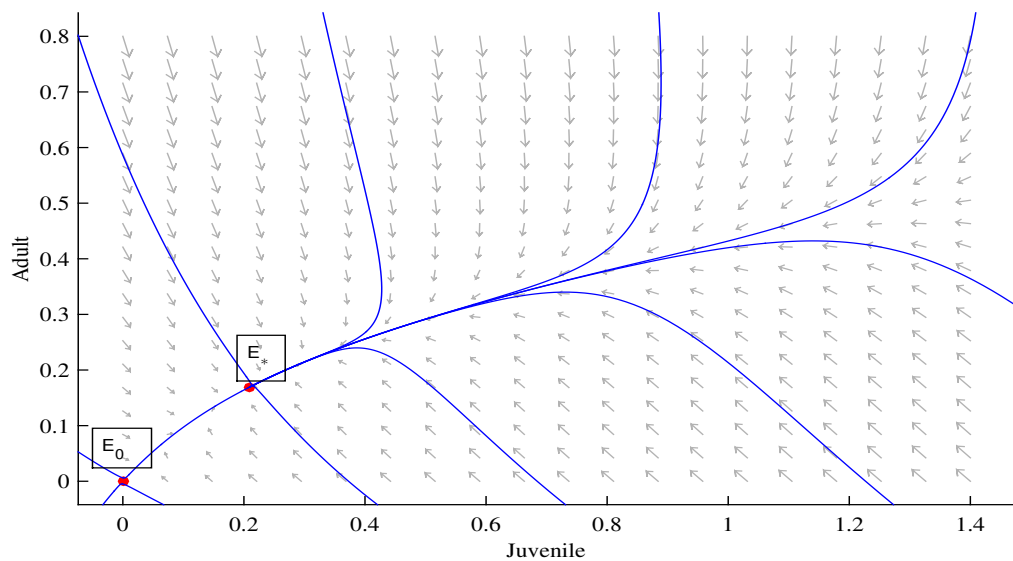


Figure 3 Phase portrait of model (22), $\alpha = 1, \beta = 0.75, \delta_1 = 0.26, \delta_2 = 0.25, \gamma = 4, \tau = 0.2$.

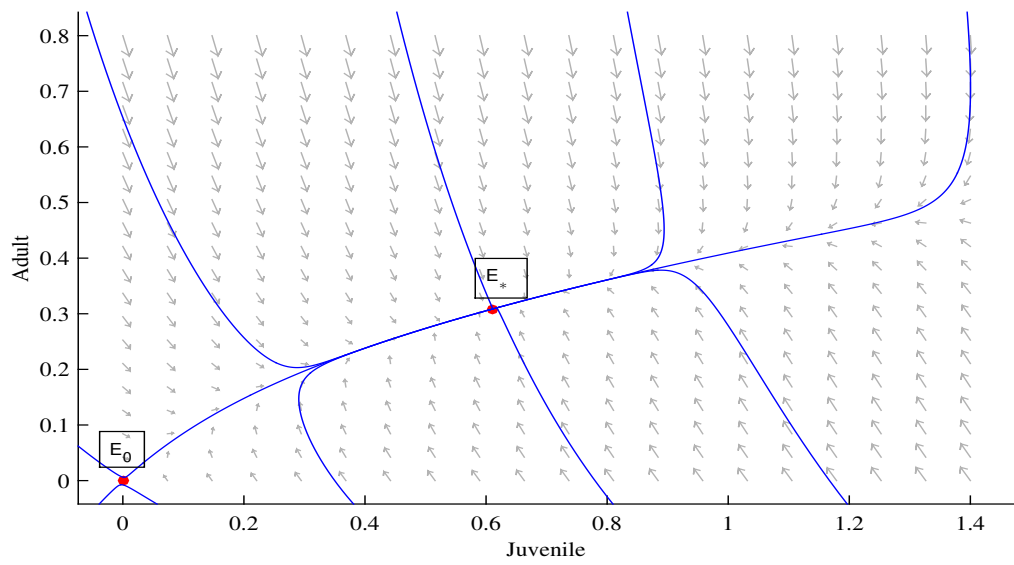


Figure 4: Phase portrait of model (22), $\alpha = 1, \beta = 0.75, \delta_1 = 0.26, \delta_2 = 0.25, \gamma = 4, \tau = 0.5$.

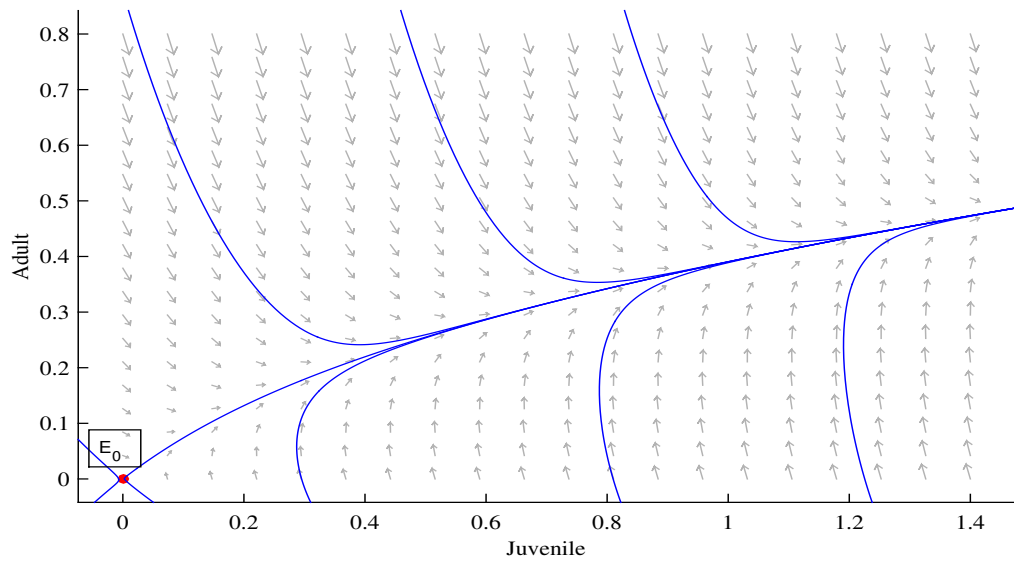


Figure 5: Phase portrait of model (22), $\alpha = 1, \beta = 0.75, \delta_1 = 0.26, \delta_2 = 0.25, \gamma = 4, \tau = 0.8$.

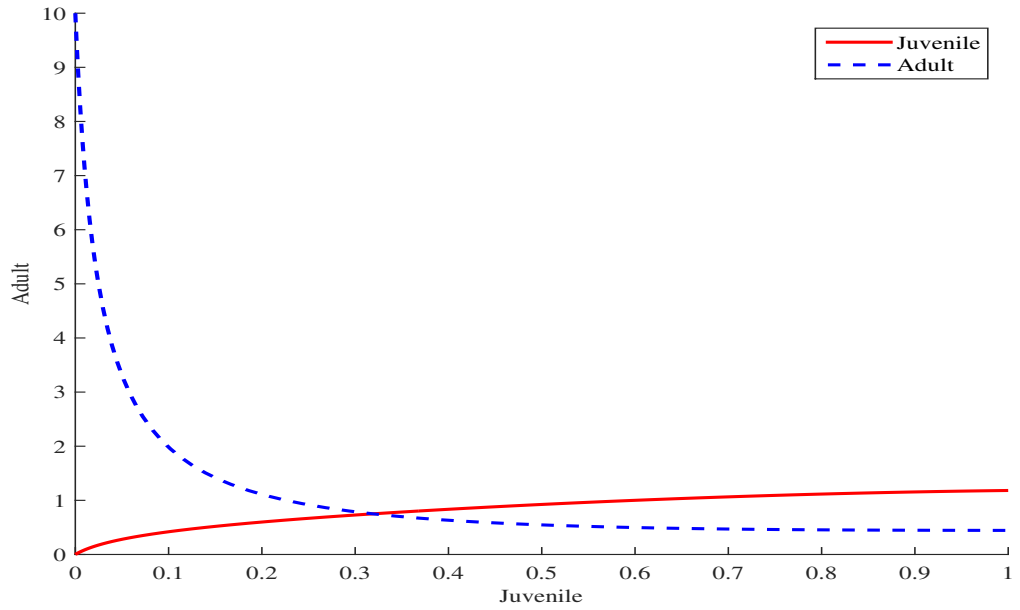


Figure 6: Simulation of model (22), $\alpha = 1, \beta = 0.75, \delta_1 = 0.26, \delta_2 = 0.25, \gamma = 4, \tau = 0.8$.

The coexisting equilibrium is locally asymptotic at E_* , according to theory (2); Figures 3, 4, and 5 corroborate this claim. Figure 6 illustrates how the growth of the juvenile is minimal having effect on the adult population growth.

Table 3: Parameters and their Values

Parameters	Descriptions	Values	Source
a	intrinsic growth of juvenile population	1	(Yu et al., 2020)
t	time of the juvenile population	1	(Yu et al., 2020)
b	Maximum attack or harvest rate	0.75	(Yu et al., 2020)
c	The half saturated level	0.26	(Yu et al., 2020)
e	Surviving rate of the juvenile population	4	(Yu et al., 2020)
τ	delay on the juvenile population @	0.2, 0.8	[Estimated]

Source: Yu *et al.*(2020)

The coexisting equilibrium point of system (24) is; $E_* = (1.3463, 1.6518)$
 which are feasible if $b < c - a = 0.26 - 1 = -0.74$

In order to verify the bistability, we compared systems (23) with (24).

Below are various different scenarios of delayed induce stability changes in the model.

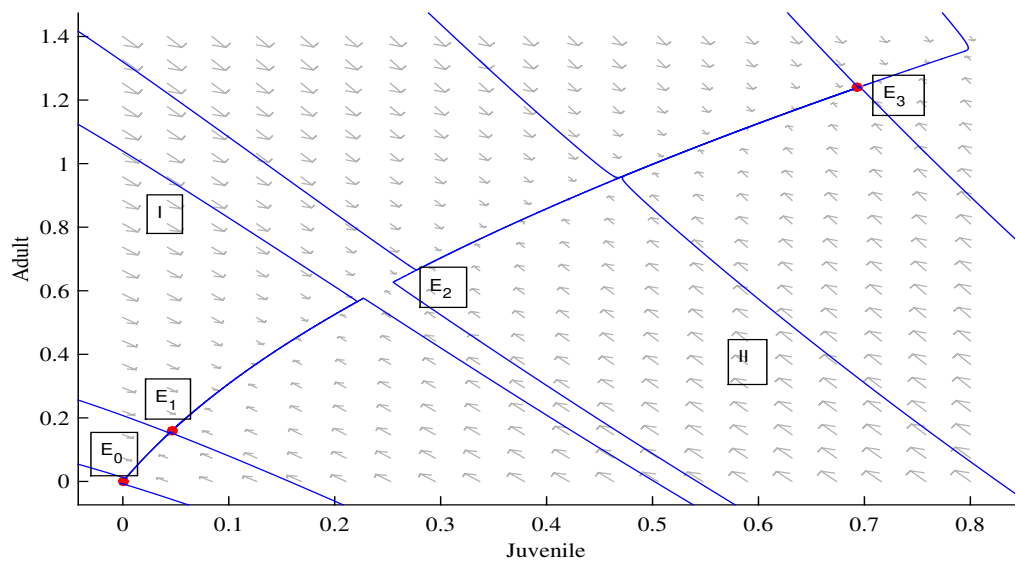


Figure 7: Phase portrait of model (23), $a = 1, b = 0.75, C = 0.26, e = 4$.

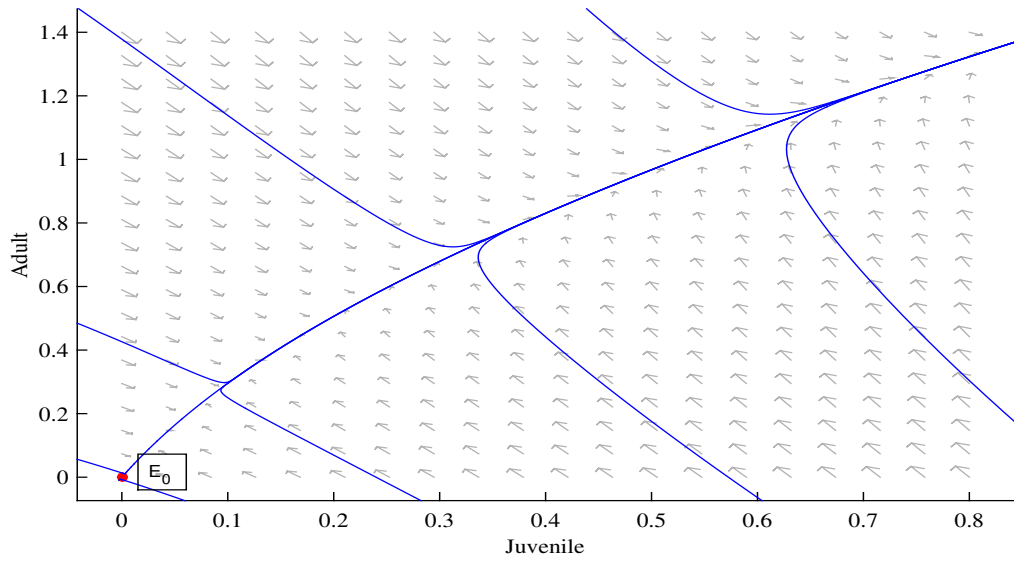


Figure 8: Phase portrait of model (24), $a = 1, b = 0.75, c = 0.26, e = 4, \tau = 0.2$.

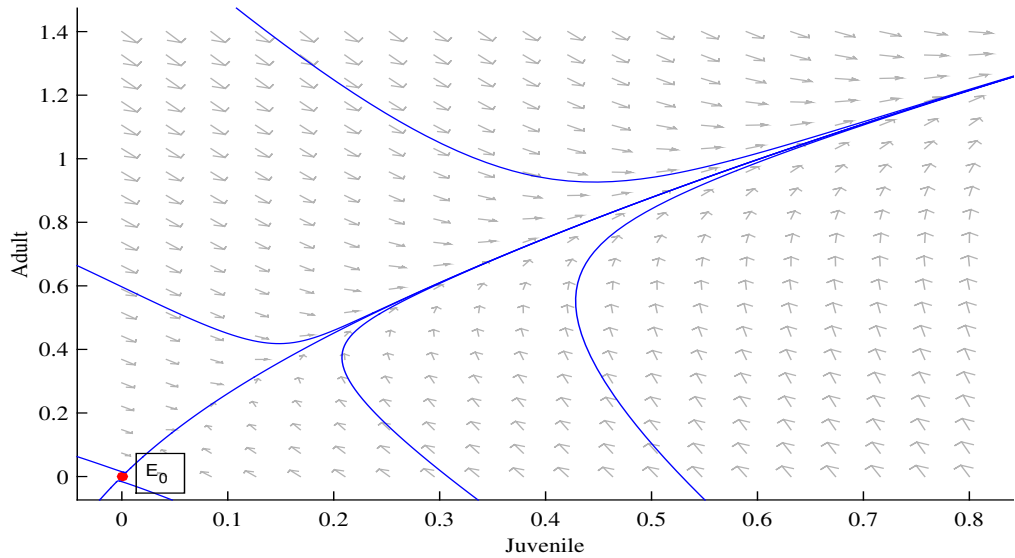


Figure 9: Phase portrait of model (24), $a = 1, b = 0.75, c = 0.26, e = 4, \tau = 0.8$.

The shapes in Figures 8 and 9 are different from Figure 7. All have a saddle point with a stable manifold; however, Figures 8 and 9 only show one quadrant, therefore the bistability shape is different. This suggests that since the juvenile and adult species would coexist in their natural habitat, the bistability will not hold true in Figures 8 and 9.

Here are several distinct scenarios of delayed induce stability changes in the model using system (23) and comparing with system (24) if $a = 1, b = 20/27, c = 7/27$, and $e = 4$.

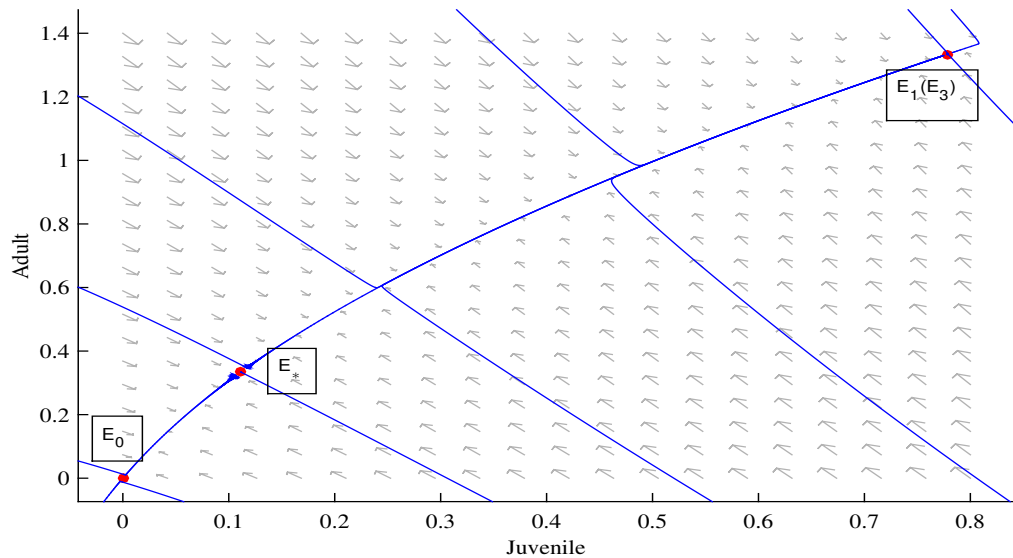


Figure 10: Phase portrait of model (23), $a = 1, b = 20/27, c = 7/27, e = 4$.

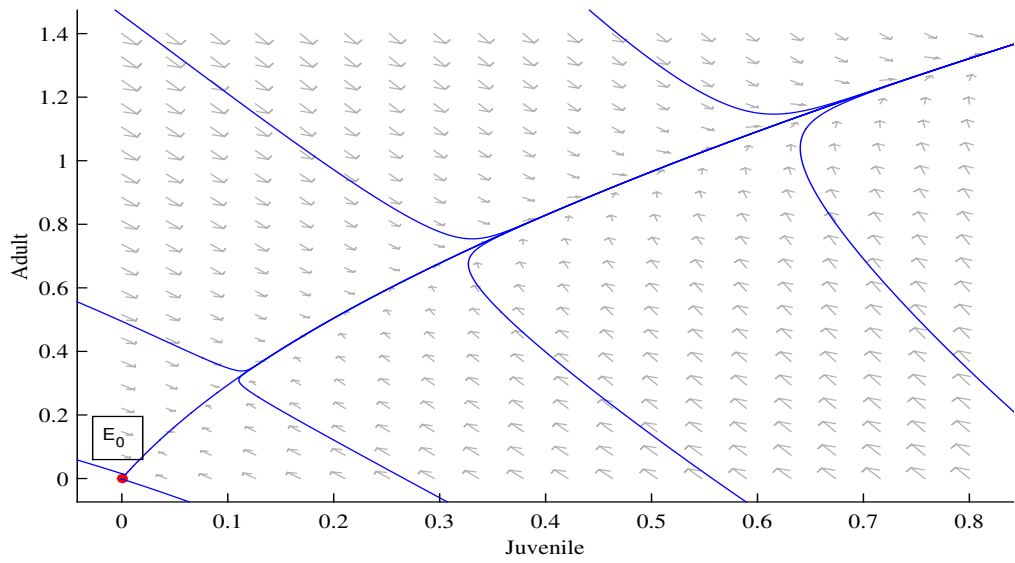


Figure 11: Phase portrait of model (24), $a = 1, b = 20/27, c = 7/27, e = 4, \tau = 0.2$.

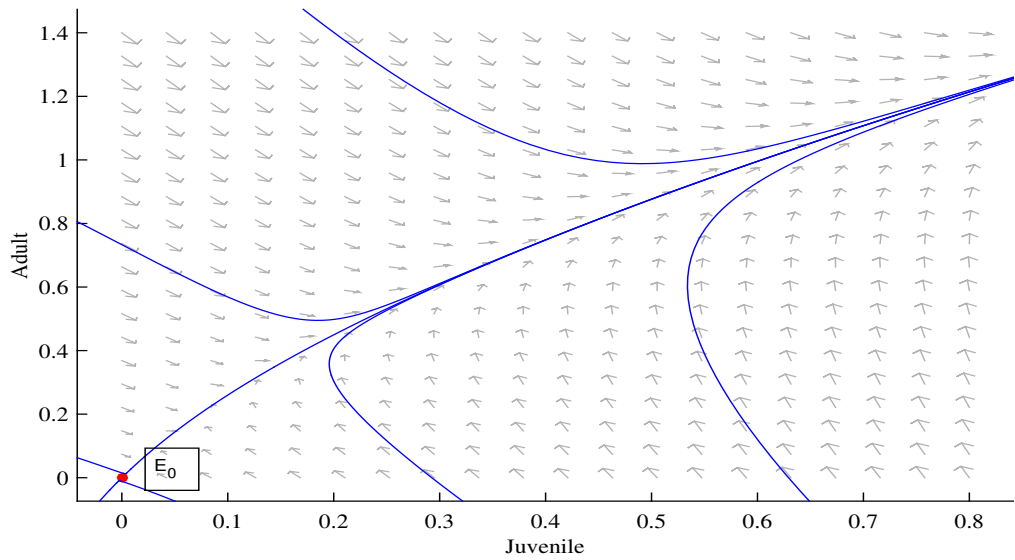


Figure 12 Phase portrait of model (24), $a = 1, b = 20/27, c = 7/27, e = 4, \tau = 0.8$.

When the delay is applied and altered, Figures 11 and 12 only have one unstable equilibrium, E_0 , but Figure 10 has two positive equilibria, E_* and E_1 (or E_3), and one unstable boundary equilibrium. This implies that while juvenile and adult may coexist in their natural habitat.

The numerical simulations of system (24) using delayed induce model, where $a = 1, b = 0.25, c = 0.125, e = 0.5$, are shown below in comparison to system (23).

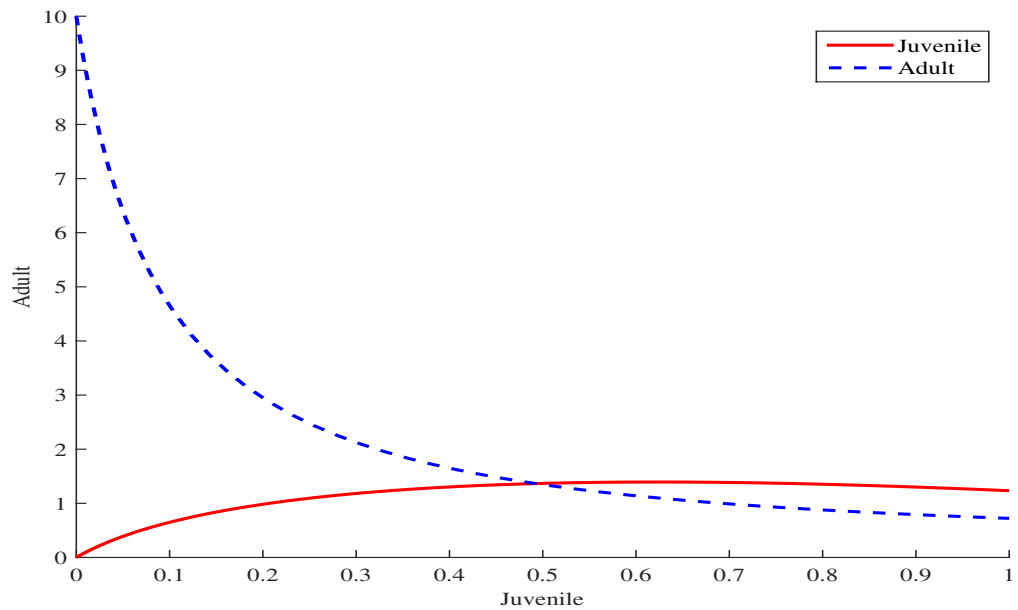


Figure 13: Simulation of model (23), $a = 1, b = 0.25, c = 0.125, e = 0.5$.

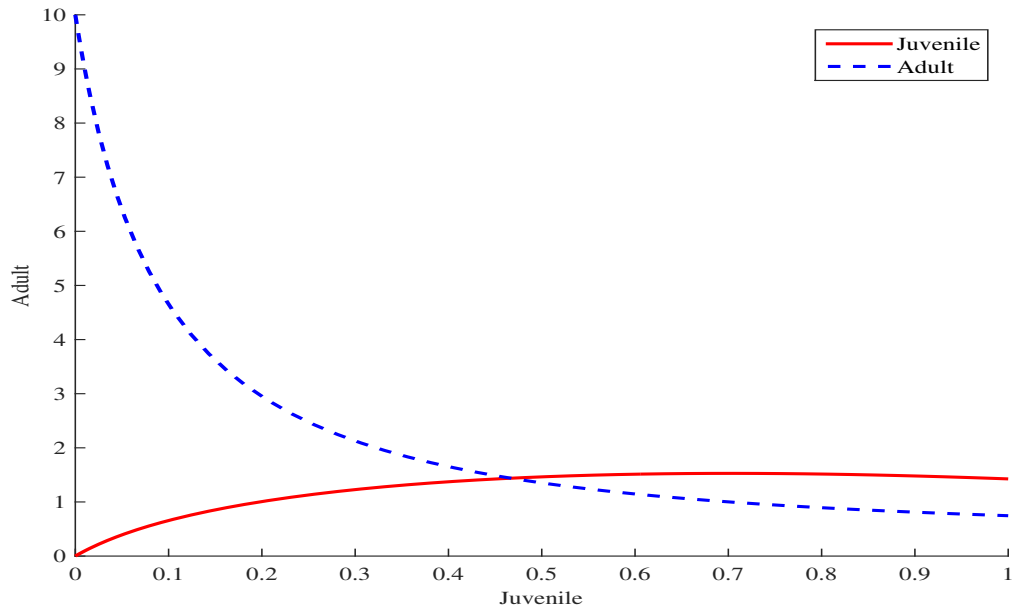


Figure 14: Simulation of model (24), $a = 1, b = 0.25, c = 0.125, e = 0.5, \tau = 0.2$.

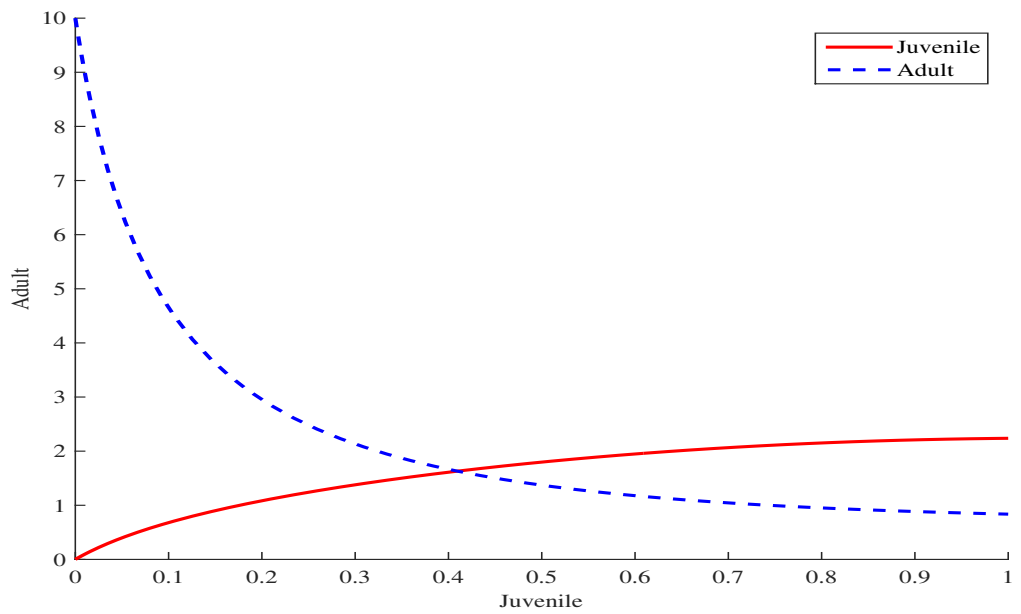


Figure 15: Simulation of Model (24), $a = 1, b = 0.25, c = 0.125, e = 0.5, \tau = 0.8$.

To confirm the potential impact of delay on Michaelis-Mentens type harvesting, let simulate using other numbers. Using system (23) and comparing with system (24) when $a = 1, b = 1, c = 12, e = 2$, and $\tau = 0.2, 0.8$.

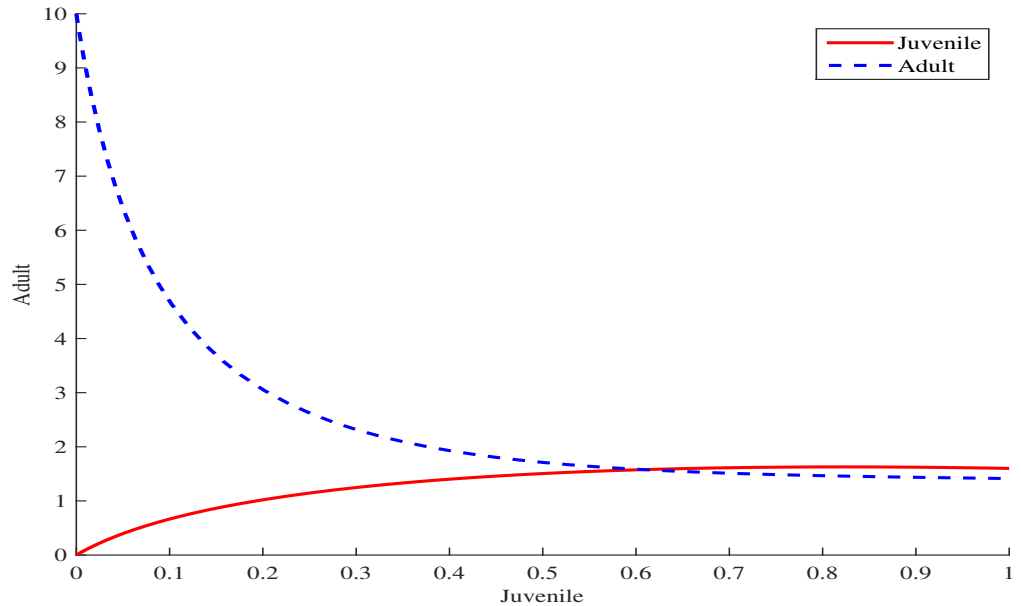


Figure 16: Simulation of model (23), $a = 1, b = 1, c = 12, e = 2$.

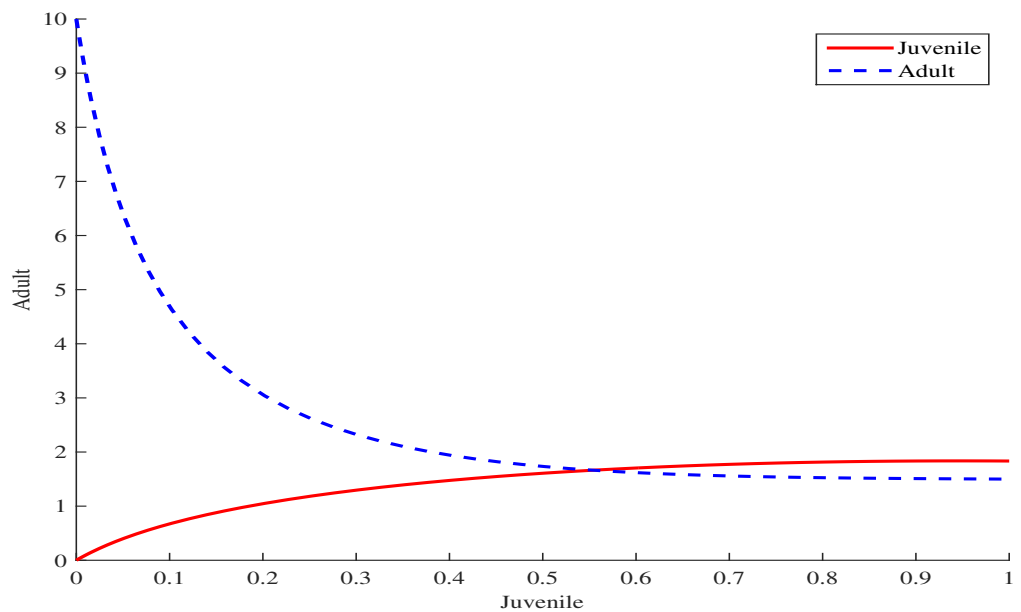


Figure 17: Simulation of model (24), $a = 1, b = 1, c = 12, e = 2, \tau = 0.2$.

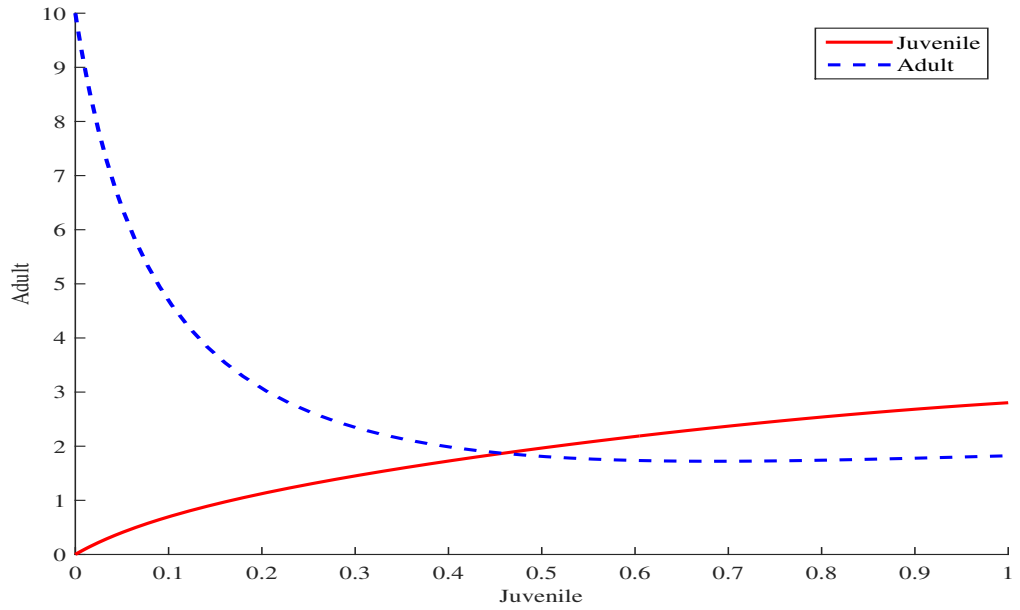


Figure 18: Simulation of model (24), $a = 1, b = 1, c = 12, e = 2, \tau = 0.8$.

Determine how the change could affect the system (24) if $a = 1, b = 0.25, c = 0.125, e = 0.5$, when $\tau = 4.71$; by choosing a number over the crucial time delay threshold for simulation. The following situations depict variations in the model's delayed induce stability:

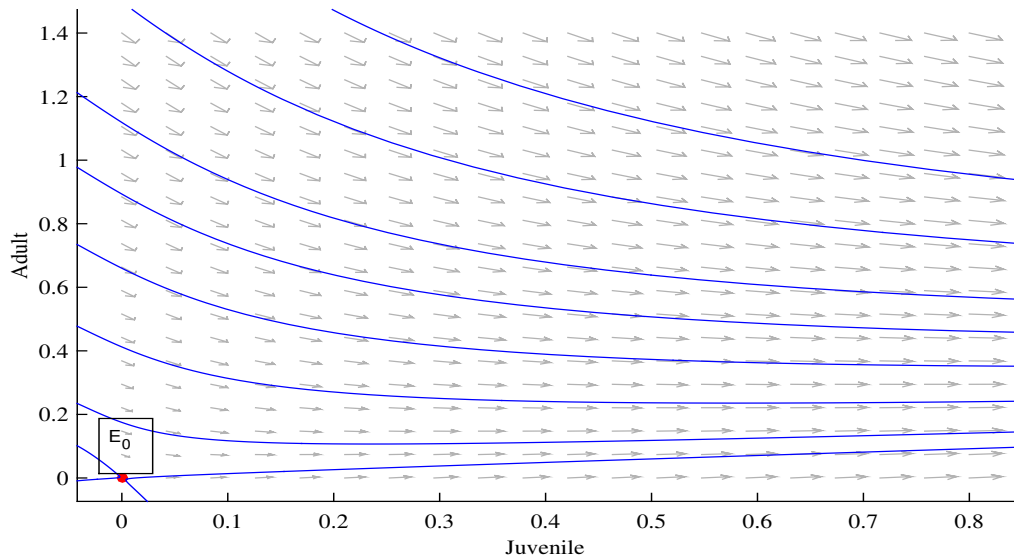


Figure 19: Phase portrait of model (24), $a = 1, b = 0.25, c = 0.125, e = 0.5, \tau = 4.71$.

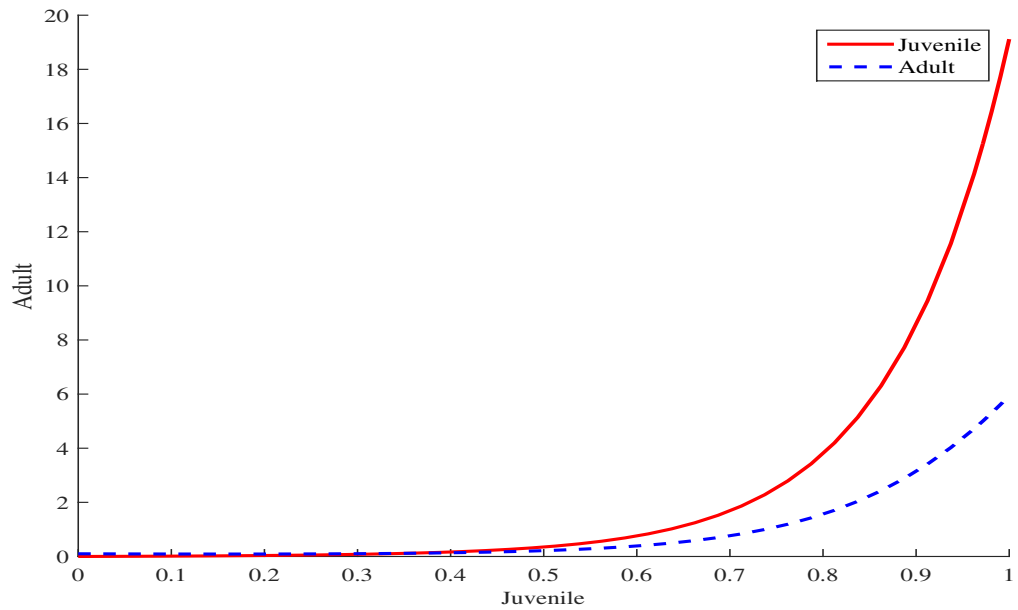


Figure 20 Simulation of model (24), $a = 1, b = 0.25, c = 0.125, e = 0.5, \tau = 4.71$.

No stability change .

At coexisting equilibrium, $E_* = (0.5, 0.7)$ of system (24) when $b = 0.25$. which shows that the system is stable in the absence of time delay. Since $C_2 : (h^2 - a^2) = (1)^2 - (2.48)^2 = -5.1504 < 0$, agreeing with **case 1**. As there exists no real ω for which $\lambda = i\omega$ is the root of system (54). Therefore, the equilibrium E_* will remain constant and no stability change will take place with respect to change in τ and this can be verified from **figure 3**. The time taken by the trajectories to converge to the equilibrium E_* increases as the value of τ increases. This implies that, the species will be stable irrespective of the time delay, and the ecosystem of the species will not be altered.

For the equilibrium E_* , the condition $C_3 : (c^2 - k^2) < 0 = [(-0.031)^2 - (2.4)^2] = -5.6694 < 0$ is satisfied, which corresponds to **Case II**. Hence there exist only one positive ω given by $\omega_{\pm} = 8.2583$, with the corresponding threshold value of τ are obtained as $0 < \tau_0^+ = 21.7963 < \tau_1^+ = 22.2746 < \tau_2^+ = 23.3179 < \tau_3^+ = 24.0788 < \dots$ The distribution of the crit-

ical thresholds of τ suggests that the equilibrium E_* is stable for $\tau < \tau_0^+$.

Stability switch.

This issue arises when a system repeatedly loses and regains stability for different parameter(s). As mentioned before, we noted that a shift in stability happened when the system parameter meet its requirements.

$C_4: (a^2 - h^2) = (2.4)^2 - (1)^2 = 4.76 > 0$ and $\sqrt{\Delta} > 0$
 $= \sqrt{[(2.4)^2 - (1)^2]^2 - 4\sqrt{(-0.301)^2 - (2.4)^2}} = 5.1504 > 0$, which aligned with **Case III**.

If $\tau = \tau_n^+$, the characteristic equation yield two distinct positives, $\omega_+ = 8.2583$, and $\omega_- = 8.1274$, the transversality condition in order to prove that the same parameter conditions also cause delay-induced stability switching, thus, if we let $b = 0.25$, the coexisting equilibrium $E_* = (0.5, 0.7)$ is saddle in the absence of time delay follows from **Case III**, hence, from system (54) with it corresponding threshold at system (73) as:

$0 < \tau_0^+ = 21.7963 < \tau_1^+ = 22.2746 < \tau_2^+ = 23.3179 < \tau_3^+ = 24.0788 < \tau_0^- = 31.0123...$ Thus, When $\tau = \tau_0^+$, E_* experiences stability, and a Hopf bifurcation takes place at E_* . Then its transversality conditions are $\Delta \neq 0$ and $\frac{d(Re\lambda)}{d\tau}|_{\tau=\tau_n^+} = 0.7924 > 0$ and $\frac{d(Re\lambda)}{d\tau}|_{\tau=\tau_n^-} = -0.7924 < 0$

The system (24) displays Hopf bifurcation around E_* when τ reaches the critical threshold τ_n^+ . A pair of conjugate complex eigenvalues cross the imaginary axis C^0 and travel from the C^+ plane to the C^- as the parameter τ increases.

$C_5: (a^2 - h^2) > 0 = [(2.4)^2 + (1)^2]^2 = 4.76 > 0$. from **Case IV** is satisfied. the two fold positive $\omega_0 = 2.38$ exist and the corresponding threshold value of τ are: $0 < \tau_0^0 = 88.6743 < \tau_1^0 = 91.7696 < \tau_2^0 = 94.8650 < \tau_3^0 = 97.9603 < ...$ The transversality condition $\frac{d(Re\lambda)}{d\tau}|_{\tau=\tau_n^0} = 43.5415 > 0$

. Consequently, the equilibrium E_* changes its behavior from stable to unstable when τ exceeds τ_0^+ .

Consequently, when τ exceeds τ_n^0 , E_* becomes unstable. These threshold values become degenerate when the eigenvalue crossing condition is not met. As τ increases through τ_n^0 , two eigenvalues from C^- contact C^0 for $\tau = \tau_n^0$. The pair of conjugate complex eigenvalues also never sit on C^0 since $\tau_n^{0'}$ s have unique values; instead, they return to C^- as soon as τ exceeds τ_n^0 .

Chapter Summary

Numerical simulation using literature values and some derived parameters were used in this chapter to test the impact of time delay on the stage structure model with Michaelis-Mentens type harvesting. The numerical simulation were performed using Matlab.

Critical threshold value of 4.71 was used to the demonstrate trajectory of the model.

CHAPTER FIVE

SUMMARY, CONCLUSIONS AND RECOMMENDATIONS

Overview

A mathematical model on the impacts of time delay on the Michaelis-Mentens Type harvesting stage structure model has been presented in this paper. Time delay ($t - \tau$) was incorporated into an existing model (Yu *et al.*, 2020) to assess the impact it has on the model. The analytical and numerical results of this model was in the preceding chapter. The results shows that, the time delay has a significant impact on the model. Because, an increase in the value of the time delay leads to an increase the quantity Juveniles and Adults which go a long way to prevent the extinction of the Juveniles.

Summary

The impacts of time delay on the Michaelis-Mentens-Type harvesting stage structure model were examined in this work. Analysis showed that in the absence of temporal delay, the system is stable around the coexisting equilibrium. But when a delay was added, the coexisting equilibrium was the seen in the following events:

- (a) the system remains stable for all time delays at a certain point and
- (b) the system undergoes stability switch.

Also, the study examined the stability and character of the equilibria of model (21). Since there is no delay and functional response, the system was asymptotically stable; both species coexist without any of them going extinct, and this can be seen in Figure 1 and 2. The model (22), was found to be asymptotically stable at E_* as seen in Figure 3 and 4, and unstable at E_0 see figure 5 as the time delay τ is increased.

Since some work have already been done on model (24) Yu *et al.* (2020). Their model demonstrates a wide range of positive stable states as well as complex dynamic behaviors. According to first type of bistability phenomena, as shown in Figure 7, the model is persistent when the initial value is in the first quadrant if $b < c(e - a), \Delta(b) < 0,$. According to second type of bistability phenomena, both species will either coexist under certain circumstances or go extinct under others. The same can be seen in Figure 10, where the model shows two positive equilibria E_* and E_1 or $E(3)$ and one unstable equilibrium at E_0 .

Model (24) was done in comparison to model (23), thus, determining effects of time delay on the model. It can be observed that Figure 8 and 9 from model (24), were asymptotically stable at E_0 and had no bistability, where both species coexist in their habitat but became unstable as time delay τ is increased from $\tau = 0.2, 0.8$. The same can be seen in Figure 11 and 12, as each τ is increased, the equilibrium points change from stable to unstable when compared with Figure 7 and 10 which show two equilibrium points. The various values for $\tau = 0.2, 0.8$ show that, the models are more asymptotically stable but become unstable or it undergo stability switching as the delay parameters τ are increased.

The results shows a mono-stability and dispersal, where there exist a stable coexisting juvenile-adult at a single equilibrium point. Meaning that time-delay has a positive impact on survival of juvenile population by promoting system-wide stability, reducing local fluctuations, and maintaining a stable equilibrium which tends to favor the juvenile population more. Hence, the time delay differential equation model exhibits much more interesting dynamical behavior compared with its corresponding differential equation without time delay.

Figure 12, of model (24) shows that, as the harvesting of juvenile populations increases or decreases, there are replica effects on the adult population due to the nature of the harvesting undertaking. In the event that the juvenile is invariant and time delay increases as in Table 3, the stable mode either stay stable, transition to an unstable mode, or experience a switch with respect to time delay. Nevertheless, the unstable mode does not reverse.

Also, depending on the delay time, the unstable mode can either remain unstable, suffer instability switch from unstable to stable to unstable, or stabilize, this can be seen in Figure 14 and 15. Where the juvenile population keeps increasing while the adult population keeps increasing by little. Therefore, the harvesting can stabilize the system depending on the proper selection of juvenile population $x(t - \tau)$. This can help determine, analytically, the range of the temporal delay for various dynamical events generated by harvesting.

Figure 16 of Model (23), shows a global asymptotically stable positive equilibrium as b is positive as compared with Figure 17 and 18. As the value of time delay τ increases, there is a positive effect on the juvenile-adult population. This also shows how stable the model is even as the parameters are varied for both model with each delay.

We also analyzed the behavior of the model (24) by Compute the critical time delay value and pick any delay value greater than what have been used $\tau = 0.2, 0.8$, to $\tau = 4.71$ see if the system will bifurcate either left or right. We found out the model bifurcate to the right and was saddle node. This can be verified from Figure 19 and 20. Meaning the time delay effect on the model was huge since the rate of rate of growth of the juvenile species was greater as compared with the adult species.

Conclusions

Stability of the model (24) can be maintained by adjusting the rate of harvesting and also increasing the parameter of τ , even when we have little control over the duration of delays in the natural world. Therefore, restricted harvesting thus reduces the possibility of large amplitude oscillation of juvenile population densities around their equilibrium levels and maintaining the coexistence of juvenile-adult populations in the ecosystem. If not, either juvenile species in the ecosystem will go extinct due to over harvesting of it, especially when the survival of adult depends largely on abundance of juveniles for the circle of reproduction to continue as stated in the earlier assumption.

In this paper, we encountered a coexisting equilibrium that undergoes a stability change, while experiencing a stability switch (or instability switching) but do not detect any situation of bistability with respect to delay τ .

Recommendations

We recommend that further studies be done to bring the system back to bistability using other methods to enhance the model for sustainability and continuous circle of the model.

REFERENCE

- Andrews, J., & McLone, R. R. (1976). Mathematical modelling. *ButterworthHeinemann*. 791–816.
- Arumugam, R., Guichard, F., & Lutscher, F. (2020). Persistence and extinction dynamics driven by the rate of environmental change in a predator–prey metacommunity. *Theoretical Ecology*, *13*(4), 629–643.
- Beddington, J., Free, C., & Lawton, J. (1976). Concepts of stability and resilience in predator-prey models. *The Journal of Animal Ecology*, 791–816.
- Boyce, M. S. (2000). Modeling predator–prey dynamics. *Research techniques in animal ecology*. Columbia University Press, New York, New York, USA, 253–287.
- Chen, F., Chen, W., Wu, Y., & Ma, Z. (2013). Permanence of a stagestructured predator–prey system. *Applied Mathematics and Computation*, *219*(17), 8856–8862.
- Chen, F., Wang, H., Lin, Y., & Chen, W. (2013). Global stability of a stage-structured predator–prey system. *Applied Mathematics and Computation*, *223*, 45–53.
- Chen, F., Xie, X., & Li, Z. (2012). Partial survival and extinction of a delayed predator–prey model with stage structure. *Applied Mathematics and Computation*, *219*(8), 4157–4162.
- Clark, C. W., & Mangel, M. (1979). Aggregation and fishery dynamics: A theoretical study of schooling and the purse seine tuna fisheries. *Fish. Bull*, *77*(2), 317–337.

- Cole, L. C. (1954). The population consequences of life history phenomena. *The Quarterly review of biology*, 29(2), 103–137.
- Cooke, K. L., & Grossman, Z. (1982). Discrete delay, distributed delay and stability switches. *Journal of Mathematical Analysis and Applications*, 86(2), 592–627. [https://doi.org/10.1016/0022-247X\(82\)90243-8](https://doi.org/10.1016/0022-247X(82)90243-8)
- Faria, T. (2001). Stability and bifurcation for a delayed predator–prey model and the effect of diffusion. *Journal of Mathematical Analysis and Applications*, 254(2), 433–463.
- Fransz, H. G. (1974). *The functional response to prey density in an acarine system*. Pudoc.
- Guo, S., & Wu, J. (2013). *Bifurcation theory of functional differential equations* (Vol. 10). Springer.
- Karaaslanlı, C. C. (2012). *Bifurcation analysis and its applications*. INTECH Open Access Publisher London, UK.
- Kuang, Y., & Smith, H. (1993). Global stability for infinite delay lotka-volterra type systems. *Journal of differential equations*, 103(2), 221–246.
- Lai, L., Yu, X., He, M., & Li, Z. (2020). Impact of michaelis–menten type harvesting in a lotka–volterra predator–prey system incorporating fear effect. *Advances in Difference Equations*, 2020, 1–22.
- Lei, C. (2018). Dynamic behaviors of a stage structure amensalism system with a cover for the first species. *Advances in Difference Equations*, 2018, 1–23.

- Lennox, R. J., Brownscombe, J. W., Darimont, C., Horodysky, A., Levi, T., Raby, G. D., & Cooke, S. J. (2022). The roles of humans and apex predators in sustaining ecosystem structure and function: Contrast, complementarity and coexistence. *People and Nature*, 4(5), 1071–1082.
- Liu, Y., Zhao, L., Huang, X., & Deng, H. (2018). Stability and bifurcation analysis of two species amensalism model with michaelis–menten type harvesting and a cover for the first species. *Advances in Difference Equations*, 2018, 1–19.
- Lv, Y., Pei, Y., & Wang, Y. (2019). Bifurcations and simulations of two predator–prey models with nonlinear harvesting. *Chaos, Solitons & Fractals*, 120, 158–170.
- Ma, Z.-h., Li, Z.-z., Wang, S.-f., Li, T., & Zhang, F.-p. (2008). Permanence of a predator–prey system with stage structure and time delay. *Applied mathematics and computation*, 201(1-2), 65–71.
- May, R. M., Beddington, J. R., Clark, C. W., Holt, S. J., & Laws, R. M. (1979). Management of multispecies fisheries. *Science*, 205(4403), 267–277.
- Mchich, R., Auger, P., & Poggiale, J.-C. (2007). Effect of predator density dependent dispersal of prey on stability of a predator–prey system. *Mathematical Biosciences*, 206(2), 343–356.
- Pati, N., & Ghosh, B. (2022). Delayed carrying capacity induced subcritical and supercritical hopf bifurcations in a predator–prey system. *Mathematics*

and Computers in Simulation, 195, 171–196. [https://doi .org/https://doi .org/10 .1016/j .matcom .2022.01.008](https://doi.org/https://doi.org/10.1016/j.matcom.2022.01.008)

- Vaidyanathan, S. (2016). Hybrid synchronization of the generalized lotkavolterra three-species biological systems via adaptive control. *Int J PharmTech Res*, 9(1), 179–192.
- Xiao, A., & Lei, C. (2018). Dynamic behaviors of a non-selective harvesting single species stage-structured system incorporating partial closure for the populations. *Advances in Difference Equations*, 1–16.
- Xu, C., Liao, M., & He, X. (2011). Stability and hopf bifurcation analysis for a lotka-volterra predator-prey model with two delays. *International Journal of Applied Mathematics and Computer Science*, 21(1), 97–107.
- Yan, X.-P., & Zhang, C.-H. (2008). Hopf bifurcation in a delayed lokta–volterra predator–prey system. *Nonlinear Analysis: Real World Applications*, 9(1), 114–127.
- Yu, X., Zhu, Z., & Chen, F. (2020). Dynamic behaviors of a single species stage structure model with michaelis–menten-typejuvenile population harvesting. *Mathematics*, 8(8), 1281.

APPENDIX

MATLAB CODES FOR THE PROJECT

```
function f = Juvenile-Adult(t,x)

a = 1;

b = 0.25;

c = 0.125;

e = 0.5;

m = 0.2;

f=zeros(2,1);

f(1)= x(2)-a*x(1)*(t-m)-(b*x(1)/(c+x(1)));

f(2)= e*x(1)-x(2)*(1+x(2));

function f = Juvenile-Adult(t,x)

a = 1;

b = 0.75;

c = 0.26;

d = 0;

e = 4;

m = 0.8

f=zeros(2,1);

f(1)= a*x(2)-(b+c)*x(1)*(t-m);

f(2)= b*x(1)-d*x(2)-e*x(2)^2;

function f = Juvenile-Adult(t,x)

a = 1;

b = 0.75;
```

```
c = 0.26;  
d = 0;  
e = 4;  
f=zeros(2,1);  
f(1)= a*x(2)-b*x(1)-c*x(1);  
f(2)= b*x(1)-d*x(2)-e*x(2)2;
```

plotting codes

```
close  
t0 = [01];  
x0 = [010];  
[t x]=ode45(@Bass,t0,x0);  
plot(t,x(:,1), 'r',t,x(:,2),'-b', 'LineWidth',2);  
xlabel('Time, (Years)')  
ylabel('Juvenile-Adult');  
legend('Juvenile', 'Adult')  
grid off  
plot(x(:,1),x(:,2)) Phase Portrait  
xlabel('Juvenile');  
ylabel('Adult');
```